8209442

Scheneweɪ:k, Philip Andrew

THE ACCURACY OF PULSED NEUTRON CAPTURE LOGS FOR RESIDUAL OIL SATURATION DETERMINATIONS

The University of Oklahoma PH.D. 1981

University
Microfilms
International 300 N. Zeeb Road, Ann Arbor, MI 48106

PLEASE NOTE:

In all cases this material has been filmed in the best possible way from the available copy. Problems encountered with this document have been identified here with a check mark __√__.

1. Glossy photographs or pages _____
2. Colored illustrations, paper or print _____
3. Photographs with dark background _____
4. Illustrations are poor copy _____
5. Pages with black marks, not original copy _____
6. Print shows through as there is text on both sides of page _____
7. Indistinct, broken or small print on several pages __✓__
8. Print exceeds margin requirements _____
9. Tightly bound copy with print lost in spine _____
10. Computer printout pages with indistinct print __✓__
11. Page(s) __________ lacking when material received, and not available from school or author.
12. Page(s) __________ seem to be missing in numbering only as text follows.
13. Two pages numbered __________. Text follows.
14. Curling and wrinkled pages _____
15. Other ____

THE UNIVERSITY OF OKLAHOMA

GRADUATE COLLEGE

THE ACCURACY OF PULSED NEUTRON CAPTURE LOGS FOR RESIDUAL OIL SATURATION DETERMINATIONS

A DISSERTATION

SUBMITTED TO THE GRADUATE FACULTY

in partial fulfillment of the requirements for the

degree of

DOCTOR OF PHILOSOPHY

BY

PHILIP ANDREW SCHENEWERK

Norman, Oklahoma

1981

THE ACCURACY OF PULSED NEUTRON CAPTURE LOGS FOR RESIDUAL OIL SATURATION DETERMINATIONS

APPROVED BY

DISSERTATION COMMITTEE

ACKNOWLEDGEMENTS

I am indebted to many people who have helped along the way to this particular goal in my life. I owe a particular debt to Dr. Roy M. Knapp, who provided me the opportunity to come back to the University. In addition, I thank him for serving as the chairman of the dissertation committee and for his encouragement and guidance over the course of this work. I am also grateful for the assistance given to me by the other members of the committee: Dr. Ronald Evans, Dr. Arthur McCray, Dr. Walter Fertl, Dr. Michael Devine and Dr. Chun-Ping Tsai. It is also appropriate to thank the Phillips Petroleum Company and the Oklahoma Mining and Mineral Resources Research Institute for providing financial support during the course of this work. Last, but certainly not least, I thank my wife, Colette, for her constant support and help in putting hubby through.

DEDICATION

To Nannie Hutchison -

who cherishes education

and who gave her approval.

ABSTRACT

Pulsed neutron capture logs have been used to determine residual oil saturations for many years. A previous study found that at low values of residual oil saturation (ROS) conventional pulsed neutron logging techniques did not have the accuracy necessary for enhanced oil recovery decision making requirements. Special log-inject-log techniques were developed in order to reduce the uncertainty in values of ROS measured with pulsed neutron capture logs. The expected accuracy of these log-inject-log techniques has been reported to be within ± 5 saturation percent.

A study of the uncertainty associated with ROS values determined with pulsed neutron capture logs was made using Monte Carlo simulation techniques. Field data was obtained from tests reported in the literature. The total uncertainty associated with saturations determined by both conventional and log-inject-log procedures involving pulsed neutron capture logs was found to be 3 to 4 times higher than previously published. This increase in uncertainty was due only to the parameters required in the interpretive equations. Additional uncertainty introduced by the log-inject-log process itself was not modeled. This fact makes the estimates in uncertainty presented here optimistic.

TABLE OF CONTENTS

LIST OF TABLES

TABLE		Page

LIST OF ILLUSTRATIONS

THE ACCURACY OF PULSED NEUTRON CAPTURE LOGS FOR RESIDUAL OIL SATURATION DETERMINATION

CHAPTER I

INTRODUCTION AND PROBLEM STATEMENT

The 1973 oil embargo forced both the people and the leadership of the United States to realize that energy shortages were a very real possibility for the future, but it has only been recently that a domestic exploration and drilling boom has taken place. This boom is primarily the result of the deregulation of crude oil prices. It is obvious to the observer, however, that at some point the new reserves being discovered during this boom time will begin to fall short of replacing oil and it will become necessary to maximize the recovery of hydrocarbons from known reservoirs.

The National Petroleum Council reported in 1976 that the crude oil discovered as of December 31, 1975 totaled 418 billion barrels.[26] They estimated that the total ultimate recovery by conventional means would be 137 billion barrels, of which 109 billion barrels had already been produced. Simple arithmetic shows that the oil left in place at the end of primary and secondary recovery amounts to 281 billion barrels, or a little over 67% of all the oil discovered up to that time. A more recent appraisal[20] shows the situation has not changed significantly since the National Petroleum Council report was written, and a great potential for enhanced oil recovery still exists.

Enhanced oil recovery, or tertiary recovery, is an attempt to recover the oil remaining in the reservoir at the end of primary and secondary recovery. This remaining oil saturation is called the residual oil saturation. Enhanced oil recovery techniques include three classes of processes: thermal, chemical and miscible. Thermal processes include steam injection and insitu combustion. The chemical techniques are surfactant, polymer, and alkaline flooding. The injection of micellar chemicals, carbon dioxide, and flue gas comprise the suite of miscible techniques. These processes have been described in the literature.[29] Not all techniques are applicable to any one reservoir, so screening criteria have been developed to determine the appropriate technique for a given set of reservoir rock and fluid characteristics.[17,29]

Hasiba et al[15] outlined the steps involved in planning an enhanced oil recovery project. They are:

1. Reservoir prospect screening based on production and injection history, geology, reservoir, and fluid properties.

2. Pre-pilot evaluation based on pressure tests and infill wells for special coring and logging procedures.

3. A field pilot test to determine recovery efficiency.

4. The commercial venture decision based upon the results of steps 2 and 3.

The ultimate decision made in the final step depends on the two key parameters (1) residual oil saturation, the amount of oil left in place at the end of primary and secondary recovery, and (2) recovery efficiency, the amount of the remaining oil which will be recovered. Residual oil saturation can be determined by several methods, the most promising of which is well logging. Well logging methods are popular because they enable the engineer to see vertical saturation profiles in the well. When used in multiple wells it is then possible to determine lateral variations in saturations. One of the most useful techniques is the pulsed neutron log-inject-log process since it can be run in both open and cased wellbores.

When a technique is used it is important to know the limitations and the overall accuracy associated with it. This is especially true of residual oil saturation determination since multimillion dollar decisions rest on this value. Some estimates of the accuracy of these techniques have been reported;[25,32,33,37] however Bond[4] has suggested that the precision of the techniques requires further study. The objective of this study is to assess the accuracy of both pulsed neutron capture logs and the special techniques developed for them in the determination of residual oil saturations. This assessment will then allow the user of these techniques to know what level of confidence can be placed in the resultant residual oil saturations.

CHAPTER II

RESIDUAL OIL SATURATION DETERMINATION

Residual oil saturation (ROS) can be determined using the following techniques:

1. Volumetric and material balances
2. Core analysis
3. Well testing
4. Single well tracers
5. Well logging

In this chapter each of the above techniques will be outlined. Included in each outline will be the assumptions that are required and an estimate of the overall accuracy of the technique.

Volumetric and Material Balances

The earliest techniques used to estimate ROS involve the combination of reservoir physical and fluid properties and production data. The approach used depends on the confidence that can be associated with this data. When the reservoir is well described a simple volumetric estimate can be applied. Generally however there is some uncertainty in the reservoir description, so the material balance method must be used.

The volumetric method involves, as its name implies, the estimation of the actual reservoir volume. When this total volume is adjusted for porosity and water saturation what remains is the volume occupied by hydrocarbons. The general form of the volumetric equation is

$$N = 7758 \cdot A \cdot h \cdot \phi \cdot (1-Sw)/Boi \qquad 2.1$$

Where N is the original oil in place. This equation can be adjusted to calculate the amount of oil left in the reservoir at the end of the producing life. When no free gas phase is present equation 2.1 becomes

$$N = 7758 \cdot A \cdot h \cdot \phi \cdot Sor/Bor \qquad 2.2$$

Cole[7] shows that ROS can be calculated by making use of the fact that

$$Nr = N - Np \qquad 2.3$$

When equations 2.2 and 2.3 are combined and solved for ROS the resultant equation becomes

$$ROS = Sor = \frac{(N-Np)Bor}{7758 \cdot A \cdot h \cdot \phi} \qquad 2.4$$

The material balance equation can be used when there is some uncertainty in the reservoir volume. The material balance equation in its most general form is

$$Np\{Bo+(Rp-Rs)Bg\} = NBoi\,\frac{(Bo-Boi)+(Rsi-Rs)Bg}{Boi} + m\left(\frac{Bg}{Bgi} - 1\right) + (1+m)\left(\frac{c_w Swc + c_f}{1-Swc}\right)\Delta p + (We-Wp)Bw \qquad 2.5$$

The equation is solved for N, the original oil in place, using the reservoir rock and fluid properties at some particular instant in its producing life. The solution requires that the average reservoir pressure must be known, as well as the reservoir production and fluid properties at that time. Other unknowns in the equation, such as water influx and gas cap size, can be determined by using the method of Havlena and Odeh.[16] Usually the equation is solved at several points over the reservoir's producing life and statistical techniques are used to smooth the data.

Both methods have one very serious drawback. Even if these approaches give accurate results of average ROS, they do not yield any qualitative or quantitative information as to the location of that saturation. An additional problem arises when average reservoir pressure is determined. That is, how representative is that pressure value? Another very real problem is the effect of neglecting pore collapse which results in optimistic estimations of ROS. Elkins[12] has presented field examples of the use of these methods which show some of the very significant real world problems with these approaches. Wyman[47] has estimated that the uncertainty in ROS determined with these techniques is greater than ± 12 saturation percent.

Core Analysis

Core analysis is the only direct method of determining in situ reservoir parameters. Murphy and Owens[25] have suggested that under certain conditions the ROS values resulting from this kind of analysis may be very close to the ROS in the formation. Elkins,[12] however, has pointed out that usually the values for ROS determined this way are less than values determined by other methods.

There are at least four major problems that can lead to erroneous values of ROS caused by the coring process itself. They are:

1. The alteration of the rock wettability by contact with the mud filtrate.
2. The release of overburden pressure which may alter porosity and permeability.
3. The flushing of the sample by mud filtrate.
4. The expulsion of the reservoir fluids from the core as it is brought to the surface.

Each of these factors can be controlled or at least minimized under certain conditions.

The drilling fluid used to cut the core plays a significant part in two of the factors listed above. In order to prevent the altering of the wettability of the rock it is wise not to use surfactants or caustic materials in the mud. Unfortunately no matter what mud is selected the core will undergo some flushing by the mud filtrate. The factors which influence the severity of this invasion are:[25]

1. The formation vertical permeability
2. Reservoir fluid properties
3. The overbalance pressure between the mud

column and the formation

4. The spurt loss of the mud

5. The rate of penetration by the bit

6. The interfacial tension between the reservoir and the mud filtrate

7. The core diameter

When the formation is not at residual oil saturation the oil will be flushed out of the core which will lead to a lower estimate of the oil in place. Even when the formation has been previously waterflooded and is at ROS it is still possible for the saturation to be reduced even further by high viscous forces which again leads to erroneous results. Jenks et al[19] found that the overbalance pressure was the major driving mechanism for flushing by the mud filtrate.

When the reservoir has been previously waterflooded and there is little or no gas in solution with the formation oil and the reservoir pressure is low the saturations determined by core analysis will be close to those in the formation. This is also the case when the reservoir contains heavy oil; however as the reservoir pressure increases then it becomes necessary to somehow prevent the expulsion of the reservoir fluids by gas expansion. A core barrel developed by Carter Oil Company (Exxon Production Research) in 1940 allows the recovery of a core under conditions of reservoir pressure.[37] At the surface the core is frozen in the barrel and then analyzed under controlled laboratory conditions. A more complete description of this type of operation may be found in the literature.[21]

Additional uncertainty is introduced by the core analysis procedure itself. Fluid saturations are determined in several ways depending on which fluid, either oil or water, saturation is to be measured. Ward and Barnwell[43] list the major techniques for the determination of ROS. They include vacuum distillation, distillation extraction, and high temperature retorting. Each of these techniques requires some knowledge of the reservoir oil type in order to make the appropriate empirical corrections.

As previously stated the values of ROS determined by core analysis tend to be the lowest values reported when several other techniques have been used. One exception to this trend is the case of heavy oil reservoirs where, because of high oil viscosities, core saturations are very close to saturations determined by other methods. Wyman[47] has estimated the overall uncertainty in ROS determined by coring and core analysis to around ± 4 saturation percent at best when using pressure coring and potentially greater than ± 12 saturation percent when using regular coring procedures.

Well Testing

Well testing methods involving pressure transient analysis can be used to estimate fluid saturations in reservoirs. Earlougher[11] shows how pressure buildup, draw-down, and interference testing can be used for estimation of ROS.

Two approaches can be used involving either single well or multi-well tests. Single well tests allow the determination of permeability which when used in conjunction with relative permeability data allow the determination of reservoir fluid saturations. Multiple well tests can be used to determine the system compressibility from which fluid saturations can be inferred.

For saturation estimation the single well tests of interest are either buildups or drawdowns. The data gathered from these tests are plotted using the methods of Horner[18] or Miller-Dyes-Hutchinson.[23] The effective permeability to oil can be estimated from

$$k_o = \frac{-162.6 q o B o \mu_o}{mh} \qquad 2.6$$

in the case of a pressure buildup test. The relative permeability to oil can be determined using

$$k_r = \frac{k_o}{k} \qquad 2.7$$

where k is known from core analysis. Using relative permeability curves also determined from core analysis the oil saturation can be estimated. Earlougher[11] shows an example calculation of this type. This type of analysis is only valid when there is no free gas phase present in the influence region of the test.

Earlougher[11] also shows how type curve matching of multiple well interference tests can be used to determine fluid saturations. The field data is plotted for type curve

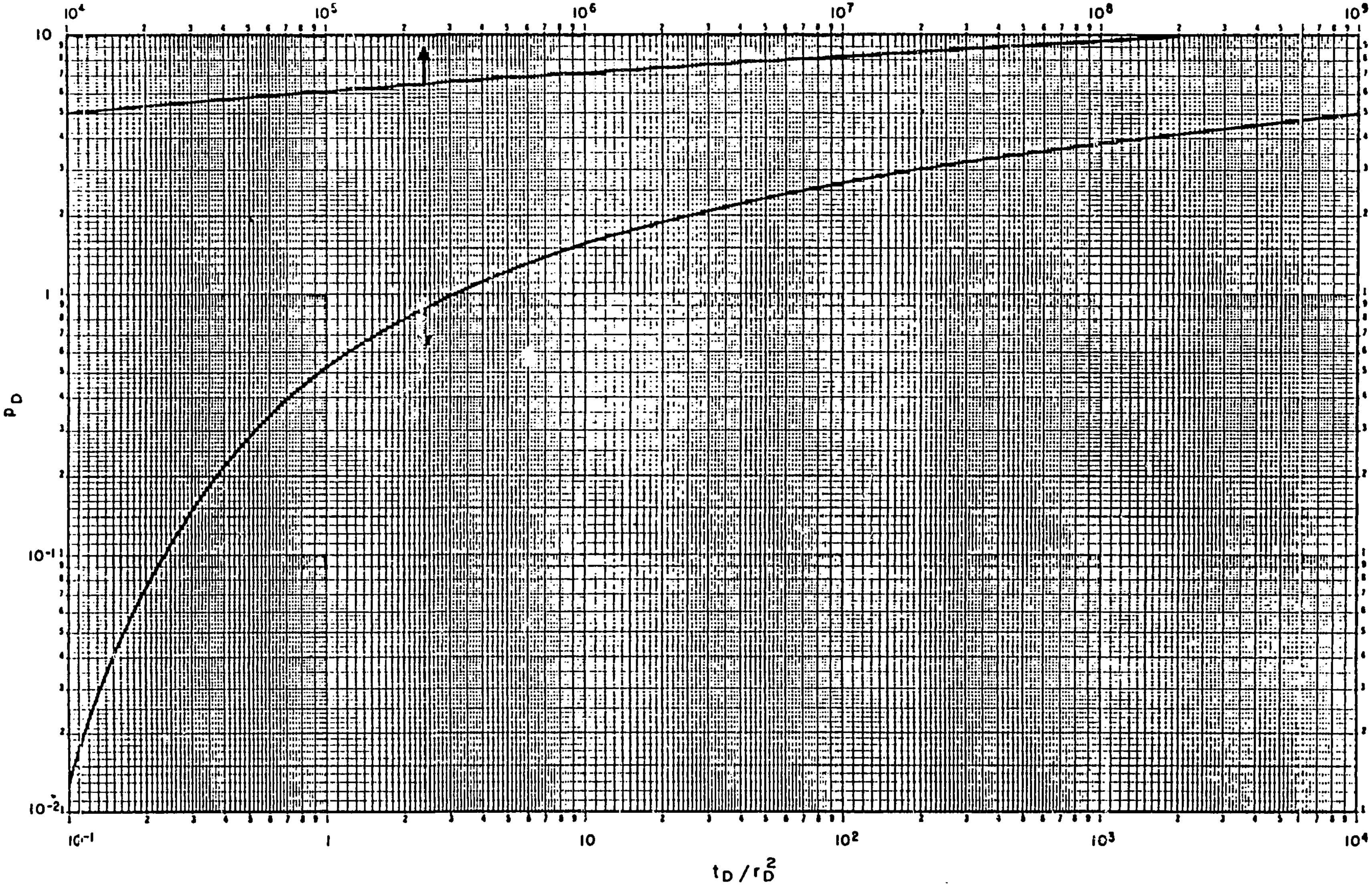

FIGURE I. Interference Testing Type Curve
(after Earlougher[11])

matching. The effective permeability of oil can be calculated from

$$k_o = \frac{141.2 q_o B_o \mu_o}{m} \frac{(\Delta p)m}{\Delta p_m}$$

where 2.8

$$\frac{(\Delta p)m}{\Delta p_m}$$

is obtained from a matching of the field data plot to an exponential integral function type curve for interference testing shown in Figure I. The total system compressibility can be estimated from

$$c_t = \frac{0.0002637(k/\mu)_t}{\phi\ r^2} \frac{\Delta t_m}{(t_d/r_d{}^2)m}$$

where 2.9

$$\frac{\Delta t_m}{(t_d/r_d{}^2)}$$

is also obtained from the type curve match. From this oil saturation can be estimated from

$$So = \frac{c_t - c_w - c_f}{c_o - c_w} \qquad 2.10$$

The reader should see Ramey[31] for an example of this procedure.

Both of these techniques have been field tested with poor results. The major problems include the sensitivity of the calculated saturations to the method of averaging core properties for single well tests and the lack of definition of total compressibility at low reservoir pressures for multi-well tests.[12] In addition, problems arise from the assumptions which are required for these methods to be valid. They include the following:[11]

1. The reservoir must be horizontal, homogenous, and isotropic with small constant total compressibility.
2. Wells being tested must be stabilized before actual testing starts and must not be influenced by other wells or reservoir boundaries.
3. All fluid saturations are uniform and no oil/water or gas/oil contacts exist.
4. The fluid properties and relative permeabilities are constant throughout the region of the test.

Wyman[47] has estimated that an overall uncertainty of greater than ±12 saturation percent exists in ROS determinations made using these techniques.

<u>Single Well Tracer Tests</u>

In a single well tracer test a tracer bank is injected into the reservoir to some desired depth of investigation. The flow is then stopped long enough for a secondary tracer to form by a chemical reaction. The well is then produced and the fluids are analyzed to determine the arrival times and quantities of the primary and secondary tracers. The value of ROS is determined using the arrival time data and a computer simulator. This procedure is described by Deans.[8]

Deans and Mojoros[9] showed that the interstitial velocity of tracer molecules flowing through two immiscible phases in a porous media could be expressed as

$$V = \frac{Vw+\beta i Vo}{1+\beta i} \qquad 2.11$$

and

$$\beta = \frac{KiSo}{1-So} \qquad 2.12$$

This describes a general chromatographic effect. The equilibrium distribution coefficient

$$Ki = \left(\frac{Ci}{Ci}\right)_{\text{equilibrium}} \qquad 2.13$$

assumes that the tracer is in local equilibrium between the two phases even though the respective velocities of v_w and v_o are different. When the oil saturation is at residual conditions then equation 2.11 becomes

$$V = \frac{Vw}{1+\beta i} \qquad 2.14$$

The simulation model with which the ROS value is determined is based on the effects of the chromatographic retardation of the primary and secondary tracers. In addition the model[9] includes the effects of:

1. Local accumulation of tracer i distributed between brine and oil,
2. Flow of the tracer away from and back to the well bore,

3. Dispersion,

4. Chemical reactions which change some of the primary tracer to secondary tracer, and

5. Fluid drift in the formation.

The most recent models[5] will also include the effects of reservoir stratification when necessary.

The chemical used for the tracer must meet the following requirements outlined by Deans.[8]

1. The primary tracer must be quantitatively distinguishable from normal reservoir components.

2. The tracer should be inexpensive, safe, and readily available.

3. The distribution coefficient should be in the range of 2-10.

4. It must not be absorbed by the reservoir rock.

5. It must react in the reservoir fluid at reservoir temperature to form a stable product.

6. The product formed should not normally be present in the reservoir fluids and its distribution coefficient should be different from the primary tracer.

Ethyl acetate is the tracer most commonly used. The ethyl acetate reacts in water to form ethanol and acetic acid. Both ethyl acetate and ethanol can be measured in concentrations as low as 0.001 percent by standard techniques.

Elkins[12] points out that there are two very real problems with single well tracer tests. They are the effects of variations of rock properties and oil saturations in the formation and the effects of brine injection on the dissolved gas content of the residual oil. Field tests have shown that the oil saturation values measured tend to be from the layers of lowest ROS,[5] when the reservoir has permeability stratifications. Wyman[47] has estimated that this method yields values of ROS to within ±8 saturation percent.

Logging Methods

Logging techniques have been used in the oil industry for many years to determine hydrocarbon saturations in old and new wells in both open and cased wellbores. Logging devices do not measure oil saturations directly but rather secondary properties of the reservoir which can be related to porosity and water saturation. While standard logging procedures may not yield satisfactory values of ROS, the newer improved techniques described here should. New devices and interpretive techniques are being developed now to further improve the accuracy of ROS determination. The logging tools of primary interest for ROS determination are resistivity and pulsed neutron capture logs. Other devices such as carbon/oxygen, nuclear magnetism, and electromagnetic propagation tools and their application to ROS determination are currently in developmental stages.

Resistivity Logs

The first tools developed for well logging were resistivity logs. These tools can be run in open hole and where the formation has been cased with a fiberglass sleeve. The interpretation of these logs is based on Archie's equation[3] which is

$$Sw = \left(\frac{FRw}{Rt} \right)^{1/n} \qquad 2.15$$

where

$$F = \frac{a}{\phi^m} \qquad 2.16$$

More complicated models have been proposed for formations which contain significant amounts of clay minerals.[38,44] Fertl[13] analyzed the uncertainty encountered in this type of evaluation of formation saturation and found that saturation exponent n, and cementation exponent m, were responsible for the largest uncertainty in ROS determined using this technique. These values are usually estimated based on the type of formation but can be determined from core analysis in order to reduce uncertainty. Even under optimum conditions ROS values calculated using resistivity devices will have uncertainties in excess of ±8 saturation percent.[13]

A log-inject-log procedure has been proposed for resistivity logs.[14,24] The technique involves the following steps:

1. Log the formation with a base resistivity log.

2. Remove the oil from the logging tool's radius of investigation using a chemical flood.

3. Resaturate the formation with formation brine.

4. Relog the formation with a resistivity log.

Using this technique the value of ROS can be determined using

$$ROS = 1 - (Ro/Rt)^{1/n} \qquad 2.17$$

The advantage of this procedure is that a large portion of the reservoir is sampled and the need for a determination of porosity has been eliminated. Fertl[13] showed that ROS could be determined to within ±4 saturation percent using this method.

There are some problems with resistivity log-inject-log procedures however. This method can not distinguish between gas and oil in the formation. In addition values of the saturation exponent n must be obtained for the entire formation from core analysis at in situ conditions. Since the effects of shale have not been studied additional work from core samples of the formation might be necessary to obtain cation exchange capacity information. This data is required for the more complex interpretation models for these logs.

Pulsed Neutron Capture Logs

Pulsed neutron capture logs can be used to determine ROS in both open and cased boreholes. There are presently two commercial systems available to the industry. A description of these tools and their theoretical basis is included as Chapter III of this work. These tools were originally designed for high porosity formations which contained high salinity formation water.

The pulsed neutron capture log measures the total or bulk capture cross section of the formation being logged. The overall response in a shale free reservoir is due to the contributions of the reservoir rock and fluids and can be expressed as

$$\Sigma t = \Sigma ma(1-\phi) + \Sigma w Sw \phi + \Sigma hc(1-Sw)\phi \qquad 2.18$$

Rearranging and solving for ROS yields

$$ROS = 1 - Sw = 1 - \frac{\Sigma t - \Sigma ma + \phi(\Sigma ma - \Sigma hc)}{\phi(\Sigma w - \Sigma hc)} \qquad 2.19$$

The values for the input parameters can be found using chemical composition data, nomograms provided by the service companies[10,35] or in the case of injection fluids measured in special tanks at the surface prior to injection.

Youmans et al[49] developed a waterflood log-inject-log process which should reduce the uncertainty in ROS determined by pulsed neutron capture logs. Using this method the uncertainties associated with the matrix and hydrocarbon capture cross sections could be eliminated. This approach involves logging the formation which results in

$$\Sigma t_1 = \Sigma ma(1-\phi) + \Sigma w_1 Sw \phi + \Sigma hc So \phi \qquad 2.20$$

Then a water of contrasting salinity is injected and the formation is relogged which yields

$$\Sigma t_2 = \Sigma ma(1-\phi) + \Sigma w_2 Sw\phi + \Sigma hcSo\phi \qquad 2.21$$

Solving Equations 2.20 and 2.21 simultaneously for ROS results in

$$ROS = 1 - Sw = 1 - \frac{\Sigma t_2 - \Sigma t_1}{\phi(\Sigma w_2 - \Sigma w_1)} \qquad 2.22$$

There are several assumptions which must be satisfied for this method to work. They are:

1. No free gas is present.
2. The formation is at residual oil saturation.
3. There is no change in oil saturation due to the injection of fluid.
4. There is no shrinkage of the reservoir oil.
5. The injection profile is radially complete and uniform.
6. The bottom hole injection pressure is below the formation factor pressure.
7. No significant shale volume is present.

This approach was attempted in a reservoir in South Louisiana and the data makes up part of this study.[32]

A second method, the chemical flood technique, has also been proposed. It involves the following steps as outlined by Richardson et al:[32]

1. Run a pulsed neutron capture log with reservoir oil and water near the wellbore.
2. Using chemical flooding techniques remove all

the oil from the formation near the well bore within the depth of investigation of the tool.

3. Inject formation water to resaturate the formation to 100 percent water saturation.

4. Relog the formation.

This results in two simultaneous equations

$$\Sigma t_1 = \Sigma ma(1-\phi) + \Sigma w Sw \phi + \Sigma hc(1-Sw)\phi \qquad 2.23$$

and

$$\Sigma t_2 = \Sigma ma(1-\phi) + \Sigma w \phi \qquad 2.24$$

Solving for ROS results in

$$ROS = So = \frac{(\Sigma t_2 - \Sigma t_1)}{\phi(\Sigma w - \Sigma hc)} \qquad 2.25$$

This technique has only been reported once in the literature and was apparently unsuccessful because of imcomplete displacement.[25]

Even using these improved techniques there is still some uncertainty in the resultant values of ROS. Robinson[33] did experimental work with an improved pulsed neutron tool in order to further reduce the uncertainty in the measurements of ROS. By making stationary readings with a tool whose source and detector spacings were increased to 80 cm. it was found that the water occupied pore volume could be determined by a waterflood log-inject-log procedure which results in

$$\phi_w = \frac{\Sigma t_2 - \Sigma t_1}{\Sigma w_2 - \Sigma w_1} \qquad 2.26$$

ROS can be determined by

$$ROS = 1 - \frac{\phi w}{\phi} \qquad 2.27$$

The field data which was taken during the test of this technique is included in this study.

Pulsed neutron capture logs have the advantage of being available for both open and cased hold determination of ROS. While Wyman[48] has indicated that these tools offer an excellent method for ROS determination, Richardson et al[32] found that at very low values of ROS the uncertainty associated with a conventional water saturation determination from pulsed neutron logs was too high to make it useful as a decision making parameter for tertiary oil recovery projects. Conventional applications of pulsed neutron logs were felt to be useful however in situations where the ROS value was on the order of magnitude of 60 saturation percent or higher. They also indicated that the expected accuracy of log-inject-log techniques using pulsed neutron tools would be in the ±5 saturation percent range.

New Developments in Logging

Early attempts at ROS determination using 4kc. carbon/oxygen logs were disappointing. This tool is a pulsed neutron device which is unaffected by changes in formation water salinity and reservoir shaliness. A recent field test[28] has shown that with both the new 20kc. tools which are now available and improved understanding of the tools' responses we can ultimately expect accurate measurements of ROS.

Nuclear magnetism logs have been available since 1960. While nuclear magnetism logs are still not a standard logging technique they have applications in the area of ROS determination. The procedure must be run in open holes of large diameters which have been drilled with special mud systems. The drawbacks of this technique are that the tools' depth of investigation is extremely shallow and the well bore data requires special processing.[48] In addition the special mud systems that are required may preclude the use of other logging techniques for ROS measurement. More work is necessary before an assessment of the accuracy of this technique can be made.

Electromagnetic propagation or dielectric constant logging for ROS determination has also been field tested.[27] It was reported that the accuracy of the reported values was limited by three factors which are listed below:

1. A lack of a unique model relating log response to saturations.
2. The uncertainty in porosity.
3. The uncertainty about electromagnetic properties of the rock matrix.

In addition there were problems with log repeatability and inaccuracy due to uneven hole diameters. Obviously much work remains to be done before use of this technique can become widespread.

CHAPTER III

PULSED NEUTRON CAPTURE LOGS

The theoretical and experimental work which lead to the development of pulsed neutron capture logs was done both in the United States and Soviet Union. The first practical logging instrument was described by Youmans et al[49] in 1963. The first tools employed a neutron source and one detector. Present tools employ two detectors but the basic principles of interpretation are the same.

The basic cycle of operation of this type of log is shown in Figure II. The electromechanical neutron source is activated for a short period which produces a short pulse of 14 mev neutrons. During the quiescent period the detectors measure the exponential decay of those neutrons and the associated neutron induced radiation as the neutrons are captured by the materials in the wellbore and formation. The capture cross section of the formation is determined from the count rates taken during two gates on the short spaced detector which is depicted in Figure II. By employing a second detector the formation porosity can be determined from the ratio of the counts from an early

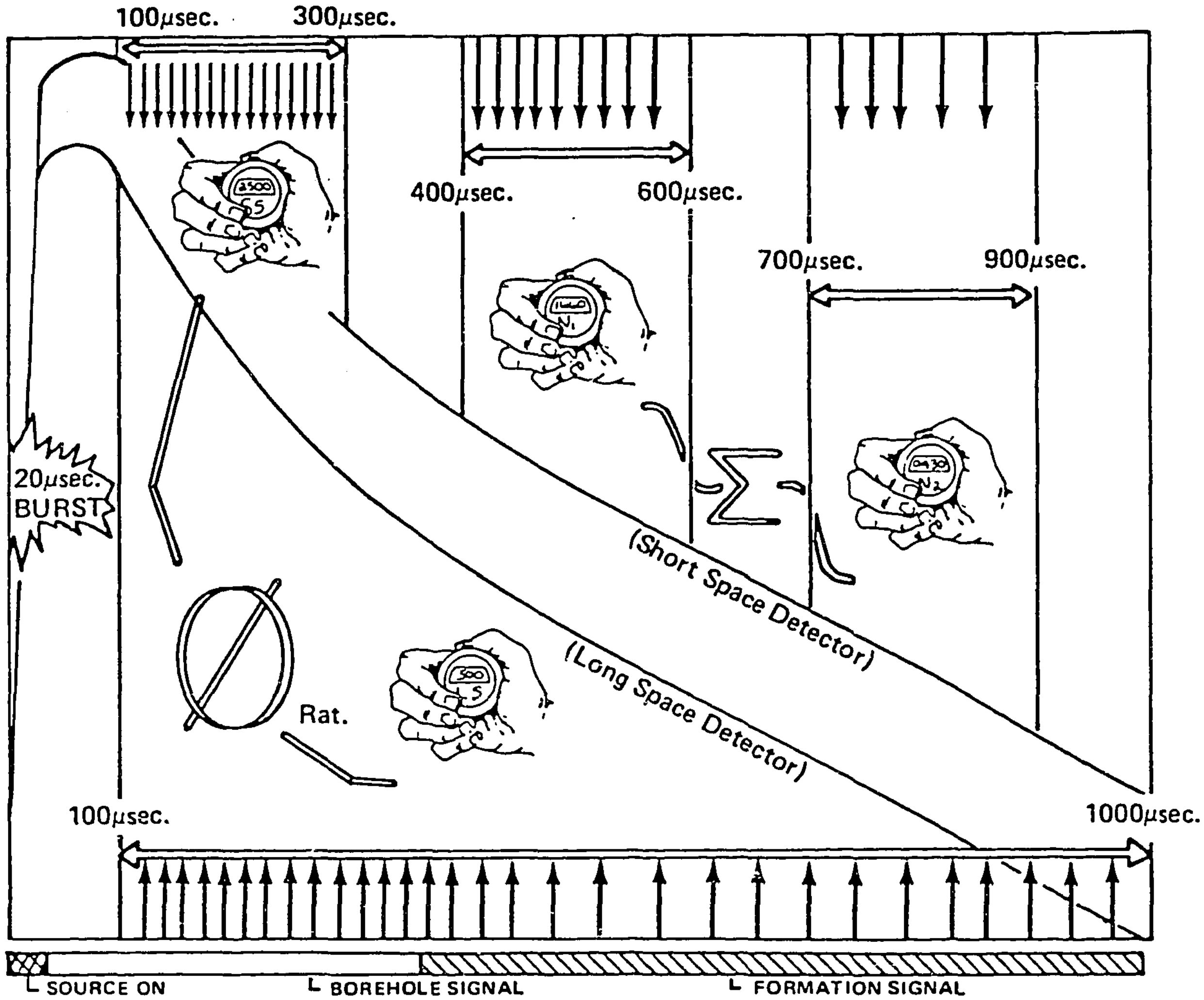

FIGURE II. Old Dual Neutron Lifetime Log Operation Cycle (after Serpas et al[36]) gate on the short space detector and the total count rate on the long space detector. This second detector is also used for interpretation in zones which are gas filled. At the present time two tools of this type are available, the Dresser Atlas Dual Neutron Lifetime Log and the Schlumberger Thermal Decay Time Log. Both of these tools operate on the same basic principles; however, there is a slight difference in the gating of the detectors which will be described later.

Pulsed neutron capture logs measure the macroscopic capture cross section Σ_t of the formation being logged. In order to derive the interpretation relationships for these logs it is first necessary to define the term "neutron lifetime". Neutron lifetime L is simply the time required for the total number of thermal neutrons existing at any instant in some medium to fall to half. This concept is similar to the half life of a radioactive element. The number of neutrons captured per unit time is proportional to the number of neutrons present. In the case of a homogeneous medium the number of neutrons present at any time is

$$N_2 = N_1 e^{-\Sigma VT} \qquad 3.1$$

The velocity of the thermal neutrons is 2200m/sec. Equation 3.1 can be evaluated using the concept of neutron lifetime where T=L and N_2/N_1=0.5 which results in

$$L = \frac{3150}{\Sigma} \qquad 3.2$$

where L has units of microseconds and Σ has the units of $10^{-3}cm^{-1}$ which is the standard capture unit.

The slope of the neutron decay curve must be known in order to determine Σ_t. As previously stated, count rates are determined at two different gates with the short spaced detector. The first gate is opened after the effects of the borehole, casing, and cement have disappeared. This is usually after about 400 microseconds. Counts are recorded for 200 microseconds. The second gate is open for 200 microseconds starting at the 700 microsecond mark in the cycle. The value of Σ_t can be determined from

$$\Sigma = \frac{10500}{\Delta T} \log \frac{N_1}{N_2} \qquad 3.3$$

where N_1 and N_2 are the count rates at gates one and two respectively. Since ΔT is usually equal to 300 microseconds, equation 3.3 reduces to

$$\Sigma = 35 \log \frac{N_1}{N_2} \qquad 3.4$$

The pulsed neutron capture log interpretation equation is based on the assumption that the bulk capture cross section Σ_t, measured by the tool, is made up of the contributions from each of the formation constituents. This can be expressed as

$$\Sigma_t = \Sigma_1 V_1 + \Sigma_2 V_2 + \ldots\ldots + \Sigma n Vn \qquad 3.5$$

For the case of a hydrocarbon bearing formation this becomes

$$\Sigma_t = \Sigma ma(1-\phi) + \Sigma w Sw \phi + \Sigma hc(1-Sw)\phi \qquad 3.6$$

When the formation contains shale the additional shale volume and resulting porosity reduction must be included which results in

$$\Sigma_t = (1-\phi-Vsh)\Sigma ma + Vsh\Sigma sh + Sw\phi_e\Sigma w + (1-Sw)\phi_e\Sigma hc \qquad 3.7$$

where ϕ_e is the effective porosity which can be expressed as

$$\phi_e = \phi - \phi \cdot Vsh \qquad 3.8$$

These devices have a 13 to 19 inch radius of investigation in normal boreholes. The borehole fluid, casing, and hole size do not adversely affect the Σ_t value but can have adverse effects on porosities determined with this tool. Normal bed resolution is on the order of 3.5 feet at normal logging speeds.[36]

Many uses have been proposed for pulsed neutron capture logs. Besides normal water saturation determination, these logs can be used for reservoir monitoring and residual oil saturation determination. Reservoir monitoring includes the determination of change in either water saturation or hydrocarbon properties over time. These logs have been used in open and cased holes as well as in drill pipe with good results.[36]

While the interpretive equations are valid for both logging tools, the actual Σ_t determination is different. The previous section described the operation of the earliest Dual Neutron Lifetime log which was used to obtain much of the field data used in this study. A more advanced processing technique allows Σ_t to be determined with less statistical variation. Randall et al[30] have shown that by determining a first pass Σ_t from a gate opened from 400 to 1000 microseconds, an improved value of Σ_t can be derived from a second gate of fixed width. It has been demonstrated that borehole effects have disappeared by 400 microseconds and exponential neutron decay has begun. When the formation has a very high Σ value, the borehole effects may disappear as early as 200 microseconds. By shifting the second fixed width gate so that it opens at an earlier time, a more accurate value of Σ_t can be obtained since the count rate statistics are improved by determining the value when the counts are more frequent. This improvement is due to the fact that background radiation becomes more pronounced during the late time portion of the neutron decay curve. The fixed width gate has a duration of 600 microseconds and starts anywhere from 200 to 400 microseconds into the cycle. The start time can be expressed as

$$T = 600 - 10.0\Sigma \qquad 3.9$$

where Σ is the first pass value. The gate can not open before 200 microseconds. This improved Σ_t determination results in better log repeatability and has now replaced the older techniques for Σ_t determination.[30]

The Thermal Decay Time Log uses a sliding gate arrangement to determine Σ_t. The amount of time that the neutron source is on and the gates are open is varied using a feedback system. A more complete description of the procedure is contained in Wahl et al.[41] Using this type of system requires corrections for borehole conditions and neutron diffusion. The available borehole corrections have been found to be inadequate which limits the accuracy of the Thermal Decay Time log.[25]

The accuracy of the Dual Neutron Lifetime log has also been questioned.[32] Wichmann[45,46] has done test pit and tank experiments which have shown that under the test conditions accurate Σ_t values were obtained without borehole and diffusion corrections. The new time derived sigma technique should further improve the accuracy of this device.[30] Bond[4] has suggested that an independent log calibration and test facility be set up to examine the precision of both types of pulsed neutron capture logs.

CHAPTER IV

MODEL DEVELOPMENT

When precise values are known for each parameter involved in any one of the equations presented for ROS determination, then a single precise value of ROS can be calculated. Unfortunately there is some uncertainty associated with each of the required parameters in all of the equations which have been presented. The uncertainty results from two sources. The first is the fact that some of the parameters are measured and there is always some uncertainty in the measurement process. The second aspect of the uncertainty is a result of the problem which arises when reservoir parameters are not known precisely and must be estimated. Walstrom et al[42] presented a method for determining the value of a function when there is uncertainty in the input parameters. This method is called Monte Carlo simulation.

In a Monte Carlo simulation a mathematical model is developed which describes the process or operation of interest. The model is then used to perform a number of repeated experiments or trials. For each trial the input parameters are sampled from their respective probability distributions in some random fashion. The experiment is performed and the trial results are analyzed using statistical techniques. This approach is used regularly in the petroleum industry to evaluate the economic attractiveness of exploration prospects, workovers, and secondary or tertiary recovery projects.[2,22,39]

Probability distributions can be used to express the uncertainty in some parameter of interest. Although many distribution functions have been proposed,[1,22] this study will use uniform and triangular distributions for variable uncertainty. The particular distribution chosen should reflect the accuracy with which the parameter is known or understood.[22]

The uniform distribution is chosen when a parameter is confined between some upper and lower limit. Every value of the parameter between those limits has an equally likely probability of occurring. Figure III shows a uniform probability density function and its associated cumulative probability function. McCray[22] showed that the cumulative probability of a parameter X is given by

$$F(X) = \frac{X-X_\ell}{X_h-X_\ell} \qquad 4.1$$

By replacing F(X) with a uniformly distributed random number R then solving for X the equation becomes

$$X = X_\ell + R(X_h-X_\ell) \qquad 4.2$$

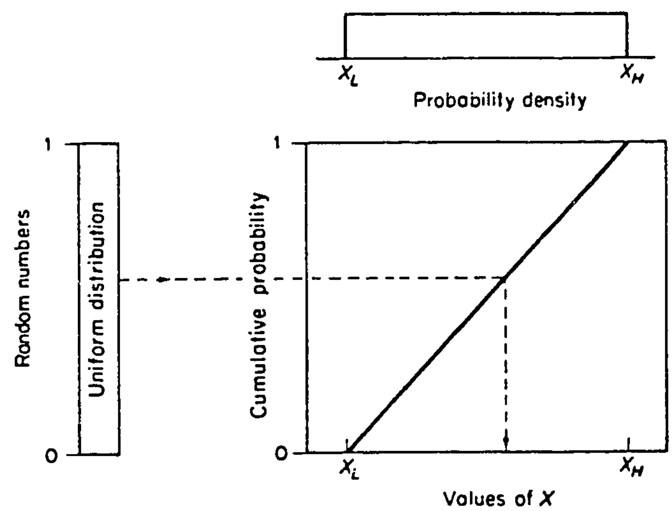

FIGURE III. Uniform Distribution and Random Value Selection (after McCray[22])

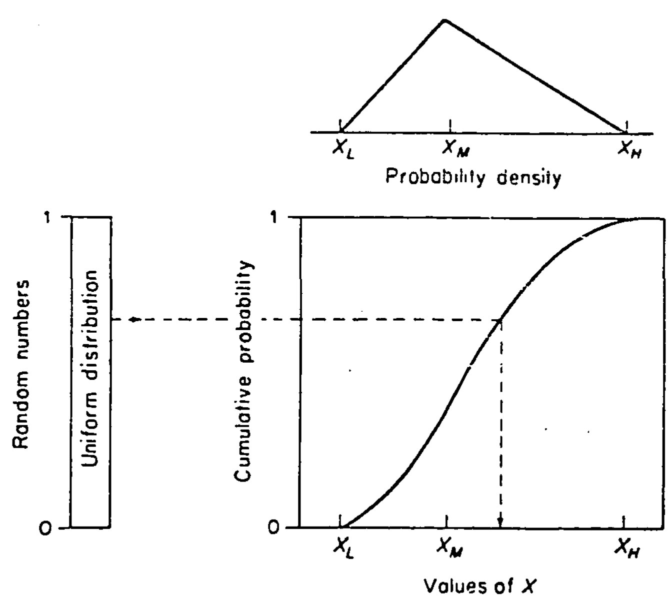

FIGURE IV. Triangular Distribution and Random Value Selection (after McCray[22])

The triangular distribution is used when a parameter has an upper and lower bound as well as a most likely value. Figure IV shows the probability density function for a triangular distribution as well as the cumulative probability function. McCray[22] showed that the cumulative probability of X is given by

$$F(X) = \left(\frac{X-X_\ell}{X_m-X_\ell}\right)^2 \left(\frac{X_m-X_\ell}{X_h-X_\ell}\right) \qquad 4.3$$

when $X_\ell \leq X \leq X_m$ and

$$F(X) = 1 - \left(\frac{X_h-X}{X_h-X_m}\right)^2 \left(\frac{X_h-X_m}{X_h-X_\ell}\right) \qquad 4.4$$

when $X_m \leq X \leq X_h$. By replacing F(X) with a uniformly distributed random number R and solving for X the equations become

$$X = X_\ell \{(X_m-X_\ell)(X_h-X_\ell)R\}^{\frac{1}{2}} \qquad 4.5$$

when $R \leq \{(X_m-X_\ell)/(X_h-X_\ell)\}$ and

$$X = X_h - \{(X_h-X_m)(X_h-X_\ell)(1-R)\}^{\frac{1}{2}} \qquad 4.6$$

when $R \geq \{(X_m-X_\ell)/(X_h-X_\ell)\}$.

In order to study the uncertainty inherent in ROS determined by pulsed neutron capture logs a Monte Carlo simulation model was developed for each of the three following cases:

1. Conventional Water Saturation Determination

$$ROS = 1 - Sw = 1 - \frac{\Sigma t - \Sigma ma + \phi(\Sigma ma - \Sigma hc)}{\phi(\Sigma w - \Sigma hc)} \qquad 2.19$$

2. Waterflood Log-Inject-Log

$$ROS = 1 - Sw = 1 - \frac{\Sigma t_2 - \Sigma t_1}{\phi(\Sigma w_2 - \Sigma w_1)} \qquad 2.22$$

3. Improved Waterflood Log-Inject-Log

$$ROS = 1 - \frac{\phi w}{\phi} \qquad 2.27$$

A chemical flood log-inject-log model was also developed but the available field data was not of sufficient quality to give representative results.[25] A sample model program is included as Appendix A.

Each simulation run consisted of 20,000 repeated trials. The number of trials was decided upon using a technique proposed by Canada and White.[6] The number of simulation trials is increased until the average value calculated approaches some nearly constant value. Figure V shows how this method works.

In order to test the validity of the general algorithm upon which each model is based, another simulation equation was used. Walstrom et al[42] presented several examples, of which one was a water saturation determination using Archie's equation. The model equation becomes

$$Sw = \left(\frac{FRw}{Rt}\right)^{1/n} \qquad 2.15$$

where

$$F = \frac{0.62}{\phi^m} \qquad 4.7$$

Using the data presented in the paper a simulation run was

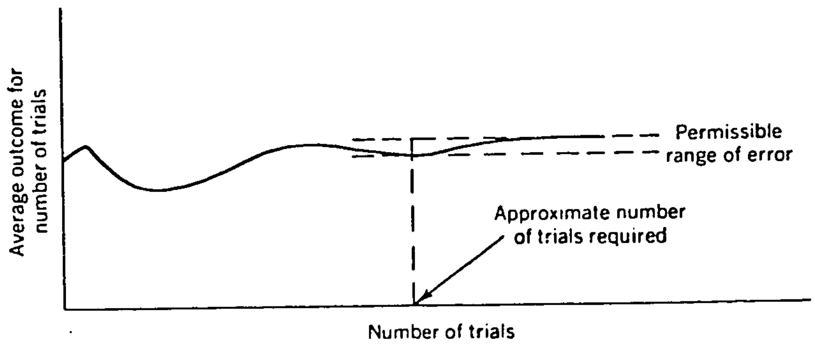

FIGURE V. Monte Carlo Algorithm Trials Optimization (after Canada and White[6])

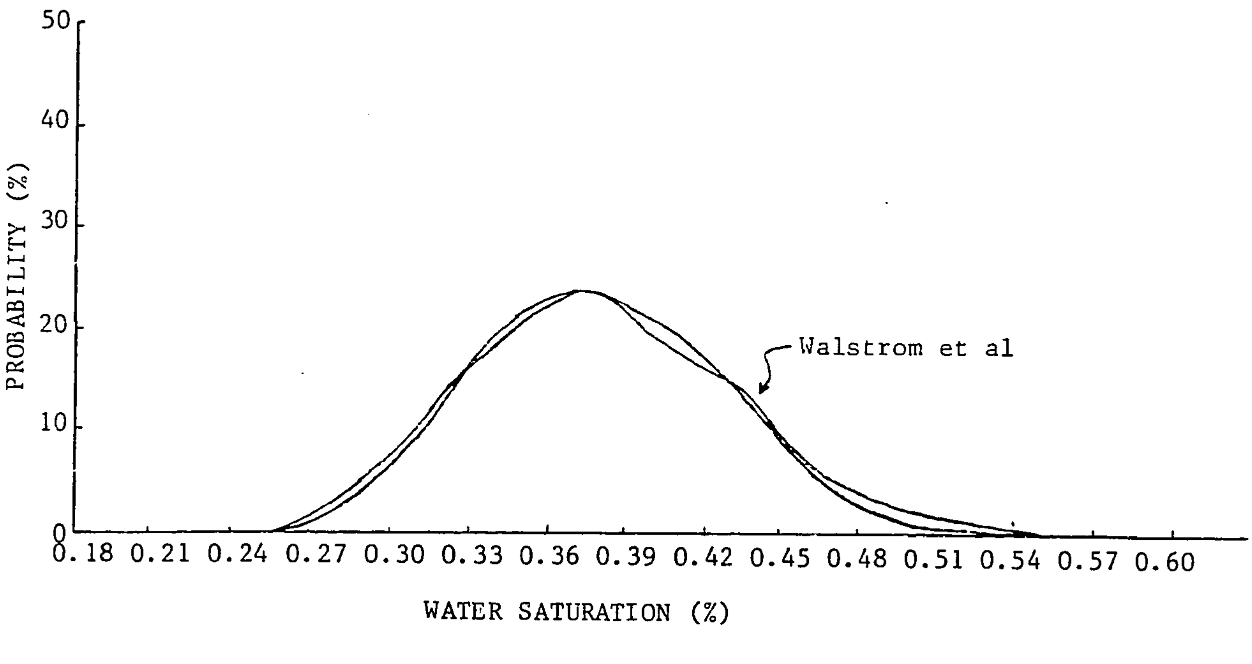

FIGURE VI. Monte Carlo Algorithm Comprarison made. The results of that run are presented in Figure VI. It can be seen that the present algorithm yields results similar to those presented by Walstrom et al.[42]

CHAPTER V

MODEL APPLICATION AND RESULTS

The Monte Carlo models developed in the previous chapter were used to simulate the field test data available in the literature. Richardson et al[32] presented data for both the conventional water saturation determination and the waterflood log-inject-log technique using pulsed neutron capture logs. These data are presented as Tables I and II respectively. Robinson[33] published data from a test of the waterflood log-inject-log procedure using an improved pulsed neutron capture log. These data are shown in Table III.

The values of each parameter and its associated uncertainty were determined in one of two ways--either by measurement or by estimation. When a parameter was measured in the field, its value was determined by multiple measurements. For example, in the conventional pulsed neutron application reported by Richardson et al[32] the value of Σ_t was determined from ten repeat passes of the logging tool over each zone. From these multiple measurements it is possible to obtain a mean value along with an associated standard deviation. If it is assumed that the parameter

Table I

Conventional Water Saturation Determination

Field Data*

Interval	Parameter	Best Estimate	Uncertainty
Zone A	Σ_t	21.6 c.u.	±1.79 c.u.
	Σ_{ma}	11.9 c.u.	±8.19 c.u.
	Σ_w	87.0 c.u.	±2.00 c.u.
	Σ_{HC}	20.5 c.u.	±0.50 c.u.
	ϕ	0.29 p.v.	±0.02 p.v.
Zone B	Σ_t	28.3 c.u.	±2.35 c.u.
	Σ_{ma}	11.9 c.u.	±8.19 c.u.
	Σ_w	87.0 c.u.	±2.00 c.u.
	Σ_{HC}	20.5 c.u.	±0.50 c.u.
	ϕ	0.29 p.v.	±0.02 p.v.

*After Richardson et al [32]

c.u. - capture unit

p.v. - pore volume

Table II

Waterflood Log-Inject-Log

Field Data*

Interval	Parameter	Best Estimate	Uncertainty
Zone 1	Σ_{t_1}	17.822 c.u.	±0.593 c.u.
	Σ_{t_2}	29.535 c.u.	±2.871 c.u.
	Σ_{W_1}	42.500 c.u.	±1.313 c.u.
	Σ_{W_2}	99.500 c.u.	±3.075 c.u.
	ϕ	0.25 p.v.	±0.01 p.v.
Zone 2	Σ_{t_1}	18.824 c.u.	±0.649 c.u.
	Σ_{t_2}	32.204 c.u.	±4.178 c.u.
	Σ_{W_1}	42.500 c.u.	±1.313 c.u.
	Σ_{W_2}	99.500 c.u.	±3.075 c.u.
	ϕ	0.27 p.v.	±0.01 p.v.
Zone 3	Σ_{t_1}	18.824 c.u.	±0.667 c.u.
	Σ_{t_2}	32.222 c.u.	±4.175 c.u.
	Σ_{W_1}	42.500 c.u.	±1.313 c.u.
	Σ_{W_2}	99.500 c.u.	±3.075 c.u.
	ϕ	0.27 p.v.	±0.01 p.v.

* After Richardson et al [32]

Table III

Improved Waterflood Log-Inject-Log

Field Data*

Interval	Parameter	Best Estimate	Uncertainty
Zone 1	Σ_{t_1}	18.070 c.u.	±0.439 c.u.
	Σ_{t_2}	27.966 c.u.	±0.739 c.u.
	Σ_{W_1}	31.532 c.u.	±0.936 c.u.
	Σ_{W_2}	73.387 c.u.	±2.172 c.u.
	ϕ	0.325 p.v.	±0.020 p.v.
Zone 2	Σ_{t_1}	16.908 c.u.	±0.615 c.u.
	Σ_{t_2}	26.639 c.u.	±0.717 c.u.
	Σ_{W_1}	31.532 c.u.	±0.936 c.u.
	Σ_{W_2}	73.387 c.u.	±2.172 c.u.
	ϕ	0.325 p.v.	±0.020 p.v.
Zone 3	Σ_{t_1}	16.588 c.u.	±0.538 c.u.
	Σ_{t_2}	28.580 c.u.	±0.825 c.u.
	Σ_{W_1}	31.532 c.u.	±0.936 c.u.
	Σ_{W_2}	73.387 c.u.	±2.172 c.u.
	ϕ	0.325 p.v.	±0.020 p.v.

* After Robinson[33]

has a normal distribution, then the end points of the parameter's range of values can be obtained by adding to and subtracting from the mean a value which is 3.09 times the standard deviation.

The value of a parameter may be estimated when it is not possible to measure it directly. When a parameter's value is estimated, it is either based on field experience or it is estimated through the use of generalized correlations. In either case the actual end points of the parameter's range are also determined by the person making the estimation. The values of Σ_w and Σ_{hc} were determined in this manner by Richardson et al.[32]

The distribution function chosen to model the uncertainty in a parameter should reflect the accuracy by which the parameter is known.[22] The triangular distribution is used when a parameter has some central tendency in its range, as is the case in a normal distribution. The application of the triangular distribution is appropriate when a parameter has been determined by repeated measurements. The uniform distribution, on the other hand, reflects less confidence in a parameter's value. The uniform distribution is used when a parameter's value has been estimated.

For each set of data from the field tests two model runs were made. These two runs were called the best and worst cases. The best case model run was made using the assumption that each parameter's uncertainty could be modeled by a triangular distribution. The worst case model was run using the uniform distribution to model the uncertainty in each parameter. When only the modeling parameters are considered, the actual uncertainty in ROS lies somewhere between the best and worst case uncertainties.

The total uncertainty in ROS may not be due to parameter uncertainty alone. The interpretive equations developed in Chapter III have some simplifying assumptions incorporated into them which may or may not be true depending on the particular field test. When the assumptions required for the interpretive equations are not true, the uncertainty may actually be higher than the worst case model indicates.

The uncertainties in ROS reported in this study are based on confidence intervals determined from the frequency distribution generated by the Monte Carlo models. The uncertainties are reported at one, five, and ten percent levels of significance. These are standard confidence levels for reporting statistical test data. In several of the field tests it is possible for certain combinations of parameter values to result in negative values of ROS which are physically meaningless. When a negative value of ROS was calculated, the model set the value to zero. Because of the problem of negative ROS values, the construction of regular confidence intervals was not possible. The confidence intervals reported in this study are based on the upper portion of the cumulative frequency distribution. For this approach to be valid, the cumulative frequency distribution must be symmetrical about the mean. When the distribution is not symmetrical the confidence intervals are only approximations for the lower portion of the cumulative frequency distribution.

In this study the uncertainty in each parameter was assumed to be independent from the uncertainty in every other parameter. For the most part this is a fairly good assumption, but there are cases where it may not be true. This might be the case when the same logging tool is used to measure multiple parameters, as in a waterflood log-inject-log test. If the tool is not properly calibrated each time a new parameter is measured, the error terms for each parameter might actually be related and should be treated as such in the modeling process.

Conventional Water Saturation Determination

The determination of water saturation using pulsed neutron capture logs involves five parameters of which only one is measured directly. The bulk sigma Σ_t is measured by the logging instrument while the matrix, water, and hydrocarbon capture cross sections must be determined from samples analyzed at the surface, from adjacent formations, or through the use of published correlations. Porosity must be known from an independent source either by core analysis or porosity logs or from both. Table IV shows the contributions of each parameter to the uncertainty of an ROS determination using this method in two different zones. To determine this contribution an end point analysis was performed for each parameter. This was done by setting all the parameters to their mean values with the exception of one. The modeling equation was then evaluated at the minimum and maximum values for the parameter of interest. This determined the range of uncertainty for that parameter. This process was repeated until all the parameters in the modeling equation had been investigated.

The largest contributors to the uncertainty in ROS are the matrix capture cross section Σ_{ma} and the true or bulk capture cross section Σ_t. The matrix cross section is the value least likely to be known. Typically a value is determined in an adjacent water zone using the logging tool and that value is then assumed to be the correct value for the zone of interest.[32] For this to be true each formation must have the same rock composition which is rarely the case. The true or bulk capture cross section of the formation is the only parameter whose range can be narrowed. This is done by making multiple passes with the logging tool over the formation of interest and then averaging the results.

The total uncertainty in an ROS measurement of this type is shown in Table V. Zone A has a fairly high value of ROS. The total uncertainty in this zone is ±29.6 and

Table IV

Conventional Water Saturation Determination

Interval	Parameter	Contribution to Uncertainty
Zone A	Σ_t	±0.094
	Σ_{ma}	±0.316
	Σ_w	±0.011
	Σ_{HC}	±0.005
	ϕ	±0.035
Zone B	Σ_t	±0.122
	Σ_{ma}	±0.316
	Σ_w	±0.022
	Σ_{HC}	±0.002
	ϕ	±0.059

Table V

Total Uncertainty

Conventional Water Saturation Determination

Interval		ROS	Uncertainty in ROS
Zone A			
	Richardson	0.63	±0.110*
	Best Case		
	10%	0.627	±0.214
	5%	0.627	±0.244
	1%	0.627	±0.296
	Worst Case		
	10%	0.627	±0.286
	5%	0.627	±0.317
	1%	0.627	±0.356
Zone B			
	Richardson	0.28	±0.120*
	Best Case		
	10%	0.280	±0.220
	5%	0.280	±0.255
	1%	0.280	±0.313
	Worst Case		
	10%	0.284	±0.299
	5%	0.284	±0.336
	1%	0.284	±0.386

*at one standard deviation

±35.6 saturation percent for the best and worst cases respectively at a confidence level of one percent. The value of ROS is much lower in Zone B. The corresponding uncertainties at a confidence level of one percent are higher at ±31.3 and ±38.6 saturation percent for the best and worst cases. Also shown in Table V are the uncertainties in ROS published by Richardson et al.[32] These uncertainties were reported at a confidence level of one standard deviation and are similar to modeled results at the same level of significance. The values of uncertainty reported by Richardson et al[32] were determined using a normal distribution for the variables in an unpublished analytical solution.*

Waterflood Log-Inject-Log

This procedure was originally proposed as a test for new reservoirs to determine the ultimate saturation change in a reservoir over its producing life.[49] It has been noted that by eliminating both the matrix and hydrocarbon capture cross sections the total uncertainty in the measurement of ROS could be lowered. This method still requires that the water capture cross sections be known either by measurement or by calculation. Porosity also must be known from an independent source. Multiple repeat logs will reduce the uncertainties of the true capture cross section Σ_t.

---

*Personal communication, J. R. Jordan, December, 1981.

The uncertainty contributions of the various parameters are shown in Table VI. In each zone the largest contributions to the uncertainty are due to the measured true formation capture cross sections of both Σ_{t_1} and Σ_{t_2} followed by porosity, ϕ. In all of the zones the uncertainty contribution to porosity is lower than would realistically be expected due to the small porosity error proposed by Richardson et al.[32] Neuman[27] showed that uncertainties in porosity are easily two percent pore volume or higher depending on the measurement technique.

The uncertainty in ROS measured by this process is shown in Table VII. The uncertainties calculated in this study are again higher that the previously reported values. This again is due to the unusual confidence interval used by Richardson et al.[32] The reduction in the porosity error coupled with the method of reporting the uncertainty combine to make this technique appear to be more accurate than it actually is. While the Monte Carlo model yields similar results at the same confidence interval, the present results are more indicative of the actual uncertainties associated with this type of test. It should also be noted that for some cases this field data yields values of ROS below zero (see Appendix B). Depending on which zone and case, the probability of this occurring could be as high as 25 percent and as low as 1 percent.

Table VI

Waterflood Log-Inject-Log

Interval	Parameter	Contribution to Uncertainty
Zone 1	Σ_{t_1}	±0.042
	Σ_{t_2}	±0.201
	Σ_{W_1}	±0.006
	Σ_{W_2}	±0.014
	ϕ	±0.033
Zone 2	Σ_{t_1}	±0.042
	Σ_{t_2}	±0.272
	Σ_{W_1}	±0.006
	Σ_{W_2}	±0.015
	ϕ	±0.032
Zone 3	Σ_{t_1}	±0.044
	Σ_{t_2}	±0.271
	Σ_{W_1}	±0.007
	Σ_{W_2}	±0.015
	ϕ	±0.032

Table VII

Total Uncertainty

Waterflood Log-Inject-Log

Interval		ROS	Uncertainty in ROS
Zone 1			
	Richardson	0.180	±0.080*
	Best Case		
	10%	0.177	±0.142
	5%	0.177	±0.163
	1%	0.177	±0.194
	Worst Case		
	10%	0.178	±0.187
	5%	0.178	±0.205
	1%	0.178	±0.233
Zone 2			
	Richardson	0.140	±0.090*
	Best Case		
	10%	0.136	±0.182
	5%	0.136	±0.209
	1%	0.136	±0.249
	Worst Case		
	10%	0.148	±0.230
	5%	0.148	±0.251
	1%	0.148	±0.281

Table VII (continued)

Interval		ROS	Uncertainty in ROS
Zone 3			
	Richardson	0.15	±0.100*
	Best Case		
	10%	0.135	±0.182
	5%	0.135	±0.209
	1%	0.135	±0.249
	Worst Case		
	10%	0.147	±0.230
	5%	0.147	±0.251
	1%	0.147	±0.281

*at one standard deviation

Improved Waterflood Log-Inject-Log

Robinson[33] devised an improved pulsed neutron device to measure ROS. The process involves the measurement of apparent neutron lifetimes in a fashion similar to that of a regular log-inject-log process. The apparent improvement in this technique is due to an increased spacing between the source and detector coupled with stationary measurements.

Examination of Table VIII shows that this improved technique has reduced the uncertainty contribution of both logging passes but porosity now becomes a major contributor. The total uncertainties for these zones are shown in Table IX. The reason for the large difference between the published data and the model results is due to the treatment of parameter uncertainty. Robinson[33] performed an end point analysis in which he neglected the uncertainty associated with porosity.

The effects of decreasing porosity are shown in Table X for the waterflood log-inject-log processes. While the data are clustered there is still a trend toward increasing uncertainty as porosity decreases. The conclusion can be made that these tools are best suited to high porosity environments.

Summary

The model results show that the uncertainties in ROS determined using pulsed neutron devices are much higher than

Table VIII

Improved Waterflood Log-Inject-Log

Interval	Parameter	Contribution to Uncertainty
Zone 1	Σ_{t_1}	±0.032
	Σ_{t_2}	±0.054
	Σ_{W_1}	±0.016
	Σ_{W_2}	±0.038
	ϕ	±0.045
Zone 2	Σ_{t_1}	±0.045
	Σ_{t_2}	±0.053
	Σ_{W_1}	±0.016
	Σ_{W_2}	±0.037
	ϕ	±0.044
Zone 3	Σ_{t_1}	±0.040
	Σ_{t_2}	±0.061
	Σ_{W_1}	±0.039
	Σ_{W_2}	±0.046
	ϕ	±0.055

Table IX

Total Uncertainty

Improved Waterflood Log-Inject-Log

Interval		ROS	Uncertainty in ROS
Zone 1			
	Robinson	0.274	±0.025
	Best Case		
	10%	0.27	±0.058
	5%	0.27	±0.067
	1%	0.27	±0.086
	Worst Case		
	10%	0.271	±0.081
	5%	0.271	±0.094
	1%	0.271	±0.116
Zone 2	Robinson	0.286	±0.026
	Best Case		
	10%	0.284	±0.061
	5%	0.284	±0.071
	1%	0.284	±0.091
	Worst Case		
	10%	0.283	±0.085
	5%	0.283	±0.099
	1%	0.283	±0.122

Table IX (continued)

Interval		ROS	Uncertainty in ROS
Zone 3			
	Robinson	0.12	±0.028
	Best Case		
	10%	0.117	±0.068
	5%	0.117	±0.080
	1%	0.117	±0.101
	Worst Case		
	10%	0.117	±0.095
	5%	0.117	±0.110
	1%	0.117	±0.137

Table X

Effects of Porosity Reduction

Improved Waterflood Log-Inject-Log

Porosity	Uncertainty in Porosity	Uncertainty in ROS*
0.345	±0.02	0.101
0.325	±0.02	0.108
0.305	±0.02	0.116

*at one percent level of significance

previously published. The models of this study have only examined the uncertainty associated with the input parameter uncertainty. Smith and Stieber[40] point out that additional uncertainty is associated with the log-inject-log process itself. Additional factors which can increase uncertainty are:

1. Incomplete displacement of the injected fluids.
2. Stripping of the residual oil.
3. Shrinkage of the residual oil.

When these factors are considered the uncertainty in this technique certainly increases. The uncertainty values reported in this study can be looked on as lower limits of the uncertainties in ROS measurements of this type.

The implications of these results are very significant. While it is well known that enhanced oil recovery projects are very expensive and risky ventures, the risk is even greater than previously thought. This additional risk must be incorporated into the overall project analysis before a commercial venture decision can be made for an enhanced oil recovery project.

CHAPTER VI

CONCLUSIONS AND RECOMMENDATIONS

In this study a consistent methodology has been used to determine the uncertainty associated with residual oil saturation determinations using pulsed neutron capture logs. The Monte Carlo modeling process is useful not only because it gives a mean value of the desired product, in this case residual oil saturation, but also because it yields distribution function information which can be used in overall project evaluation. In the future, uncertainties in ROS should be reported using recognized statistical levels of confidence in order to facilitate comparison between ROS determination methods.

From the results of this work, the following conclusions can be made:

1. Accurate values of matrix capture cross sections are required when using conventional techniques to determine ROS with pulsed neutron logs. This value is critical when ROS is very low.
2. At a one percent level of significance the

uncertainties associated with ROS determinations made with pulsed neutron logs using conventional techniques are 3 times higher than previously published.

3. At a one percent level of significance the uncertainties associated with ROS determinations made with pulsed neutron log-inject-log techniques are nearly 3 times higher than previously published.

4. At a one percent level of significance the uncertainties associated with ROS determinations made with improved pulsed neutron tools are approximately 4 times higher than previously published.

5. As porosity decreases the uncertainties in ROS increase in log-inject-log procedures involving pulsed neutron logs.

6. Tool improvements can only reduce the uncertainty in ROS to a certain value. This is because the interpretive equations still require porosity information which becomes the limiting factor in the overall accuracy.

When all ROS determination techniques are placed under this scrutiny, our understanding of their accuracy will change. The implication of this study is that enhanced oil recovery projects are much riskier than previously thought. The result is that it might become necessary for oil companies to place enhanced oil recovery projects in the same risk category as exploration projects.

Further study is recommended in the following areas:

1. The magnitude of the effects of shrinkage, stripping, and non-uniform and incomplete displacement on the uncertainty in ROS measured with pulsed neutron log-inject-log procedures must be determined.
2. Other residual oil saturation determination methods should be studied using the techniques proposed in this study in order to make valid comparisons between ROS determination methods.
3. As additional field test data become available an assessment should be made of the potential of carbon/oxygen, nuclear magnetism, and resistivity log-inject-log procedures to determine ROS.
4. Since porosity is a crucial factor in the interpretive equations of all well logging methods, work should be done to reduce the uncertainty in this measurement.

BIBLIOGRAPHY

1. Aguilera, R., "The Uncertainty of Evaluating Original Oil in Naturally Fractured Reservoirs," Trans., SPWLA 19th Logging Symposium, El Paso, 1978.

2. Anderson, M. L., "Application of Risk Analysis to Enhanced Recovery Pilot Testing Decisions," J. Pet. Tech. 31 (December, 1979):1525-30.

3. Archie, G. E., "The Electrical Resistivity Log as an Aid in Determining Some Reservoir Characteristics," Trans., AIME (1942) 146, 54.

4. Bond, D. C., Study of the Potential for Future Work on Methods of Determining Residual Oil-Final Report, DOE/BETC-0007-3, 1979.

5. Bragg, J. R.; Hoyer, W. A.; Lin, C. J.; Humphrey, R. A.; Marei, J. A.; and Kolb, J. E., "A Comparison of Several Techniques for Measuring Residual Oil Saturation," SPE 7074, presented at 5th Symposium on Improved Oil Recovery, Tulsa, 1978.

6. Canada, J. R., and White, J. A., Capital Investment Decision Analysis for Management and Engineering. Englewood Cliffs: Prentice Hall, 1980.

7. Cole, F. W., "Volumetric Methods and Production Data," in Determination of Residual Oil Saturation, pp. 77-78. Edited by L. Elkins. Oklahoma City: Interstate Oil Compact Commission, 1978.

8. Deans, H. A., "Single Well Tracer Methods," in Determination of Residual Oil Saturation, pp. 156-175. Edited by L. Wlkins, Oklahoma City: Interstate Oil Compact Commission, 1978.

9. Deans, H. A., and Majors, S., The Single Well Chemical Chemical Tracer Method for Measuring Residual Oil-Final Report, DOE/BC/20006-18, 1980.

10. Dresser, Atlas. Log Interpretation Charts. Houston: Sewaawe Atlas, 1979.

11. Earlougher, R. C. Jr., "Well Testing Methods," in Determination of Residual Oil Saturation, pp. 117-155. Edited by L. Elkins. Oklahoma City: Interstate Oil Compact Commission, 1978.

12. Elkins, L. F., "Evaluation," in Determination of Residual Oil Saturation, pp. 177-261. Edited by L. Elkins. Oklahoma City: Interstate Oil Company Commission, 1978.

13. Fertl, W. H., "Determination of Residual Oil Saturations From Geophysical Well Logs in Tertiary Recovery Projects," Energy Sources 4 (No. 3, 1979): 259-280.

14. Fertl, W. H., and Reynolds, E. B., U. S. Patent No. 3,873,890, 1973.

15. Hasiba, H. J.; Wilson, L. A.; and Martinelli, J. W., "How to Organize and Plan Enhanced Recovery Efforts," World Oil 183 (January, 1977):91-95.

16. Havlena, D., and Odeh, A. S., "The Material Balance Equation as a Straight Line," J. Pet. Tech. 15 (August, 1963):896-900.

17. Hernkel, J., Projections of Enhanced Oil Recovery, 1985-1995, DOE/EIA-0183/11, 1979.

18. Horner, D. R., "Pressure Build Up in Wells," Proc., Third World Pet. Cong., The Hague, Sec. II:503-523.

19. Jenks, L. H.; Huppler, J. D.; Morrow, N. R.; and Salathid, R. A., "Fluid Flow Within a Porous Media Near a Diamond Core Bit," J. Can. P. T. 7 (Oct.-Dec., 1968):172-180.

20. Katz, M. L., "Production From E.O.R. Projects Will Increase Rapidly in the '80s," World Oil 190 (June, 1980):159-164.

21. Koepf, E. H., "Coring Methods," in Determination of Residual Oil Saturation, pp. 13-35. Edited by L. Elkins. Oklahoma City: Interstate Oil Compact Commission, 1978.

22. McCray, A. W., Petroleum Evaluations and Economic Decisions. Englewood Cliffs: Prentice Hall, 1975.

23. Miller, C. C.; Dyes, A. B.; and Hutchinson, C. A. Jr., "The Estimation of Permeability and Reservoir Pressure From Bottom Hole Pressure Build-Up

Characteristics," Trans., AIME (1950) 189:91-104.

24. Murphy, R. P. and Froning, J. R., U. S. Patent No. 3,825,752, 1974.

25. Murphy, R. P. and Owens, W. W., "The Use of Special Logging and Coring Procedures for Defining Reservoir Residual Oil Saturations," J. Pet. Tech. 25 (July, 1973):841-850.

26. National Petroleum Council, Enhanced Oil Recovery: An Analysis for Enhanced Oil Recovery From Known Fields in the United States 1976-2000, National Petroleum Council, 1976.

27. Neuman, C. H., "Logging Measurement of Residual Oil, Rangely Field Colorado," SPE 8844, presented at 1st SPE/DOE Symposium on Enhanced Oil Recovery, Tulsa, 1980.

28. Neuman, C. H., "Cased Hole Measurement of Residual Oil-San Joaquin Valley California," SPE 9918, presented at California Regional SPE Meeting, 1981.

29. Poettmann, F. H. ed. Secondary and Tertiary Oil Recovery Processes. Oklahoma City: Interstate Oil Compact Commission, 1974.

30. Randall, R. R.; Fertl, W. H.; and Hopkinson, E. C., "Time Derived Sigma for Pulsed Neutron Capture Logging," SPE 9614, presented at Bahrain SPE Meeting, 1980.

31. Ramey, H. J. Jr., "Interference Analysis for Anisotropic Formations - A Case History," J. Pet. Tech. 27 (October, 1975):1290-1298.

32. Richardson, J. E.; Wyman, R. E.; Jordan, J. R.; and Mitchell, F. R., "Methods for Determining Residual Oil With Pulsed Neutron Capture Logs," J. Pet. Tech. 25 (May, 1973):593-606.

33. Robinson, J. D., "Neutron Decay Time in the Subsurface: Theory, Experiment, and Application to Residual Oil Determination," SPE 5119, presented at 49th Fall SPE Meeting, Houston, 1974.

34. Robinson, J. D.; Loren, J. D.; and Vajnar, E. A., "Determining Residual Oil With the Nuclear Magnetism Log," J. Pet. Tech. 26 (February, 1974): 226-236.

35. Schlumberger, Departure Curves for the Thermal Decay Time Log. Houston: Schlumberger, 1976.

36. Serpas, C. J.; Wichmann, P. A.; Fertl, W. H.: DeVries, M. R.; and Randall, R. R., "The Dual Detector Neutron Lifetime Log - Theory and Practical Applications," Trans., SPWLA 17th Logging Symposium, Houston, 1972.

37. Sewell, B. W., "The Carter Pressure Core Barrel," API Drilling and Production Practice (1939):69-78.

38. Simandoux, P., "Dielectric Measurements in Porous Media and Applications to Shaley Formations," paper presented at the Symposium of the French Association of Research on the Techniques of Drilling and Production, Paris, June, 1963.

39. Smith, M. B., "Probability Models for Petroleum Investment Decisions," J. Pet. Tech. 22 (May, 1970):543-550.

40. Smith, T. J. and Stieber, S. J., "Determination of Residual Oil Saturation with Pulsed Neutron Logs - A Field Experiment," SPE 5120, presented at 49th Fall SPE Meeting, Houston, 1974.

41. Wahl, J. S.; Nelligan, W. B.; Frentrop, A. H.; Johnstone, C. W.; and Schwartz, R. J., "The Thermal Neutron Decay Time Log," Soc. Pet. Eng. J. 10 (December, 1970):365-379.

42. Walstrom, J. E.; Mueller, T. D.; and McFarlane, R. C., "Evaluating Uncertainty in Engineering Calculations," J. Pet. Tech. 19 (December, 1967):1595-1603.

43. Ward, C. E. and Barnwell, J. L., Industrial Survey of Core Handling, Storage, and Analysis Procedures for ROS Measurements - Final Report, DOE/BC/10022-6, 1980.

44. Waxman, M. H. and Smits, L. J. M., "Electrical Conductivity in Oil Bearing Shaley Sands," Soc. Pet. Eng. J. 8 (June, 1968):107-122.

45. Wichmann, P. A., "Notes on the Accuracy of Neutron Lifetime Measurement," Trans., SPWLA 13th Logging Symposium, Tulsa, 1972.

46. Wichmann, P. A., "A Short Note on the Accuracy and Linearity of the Neutron Lifetime Response,"

Trans., SPWLA 14th Logging Symposium, Lafayette, 1973.

47. Wyman, R. E., "How Should We Measure Residual Oil Saturation," Bull. Canadian Petroleum Geology 25 (May, 1977):233-270.

48. Wyman, R. E., "Logging Methods," in Determination of Residual Oil Saturation. Edited by L. Elkins. Oklahoma City: Interstate Oil Compact Commission, 1978.

49. Youmans, A. H.; Hopkins, E. C.; Bergen, R. A.; and Oshry, H. L., "Neutron Lifetime a New Nuclear Log," J. Pet. Tech. 16 (March, 1964):319-328.

APPENDICIES

APPENDIX A

```
//nanook job          ,'pschenew',class=j,time=(1,30)
// exec fortgclg
//fort.sysin dd *
cccccccccccccccccccccccccccccccccccccccccccccccccccccccccccccccccccccc
cccccccccccccccccccccccccccccccccccccccccccccccccccccccccccccccccccccc
ccccccccc                                                  ccccccccccc
ccccccccc   This program is a monte carlo simulation       ccccccccccc
ccccccccc    of the saturation equation for pulsed         ccccccccccc
ccccccccc    neutron tools.                                ccccccccccc
ccccccccc                                                  ccccccccccc
cccccccccccccccccccccccccccccccccccccccccccccccccccccccccccccccccccccc
cccccccccccccccccccccccccccccccccccccccccccccccccccccccccccccccccccccc
c
c
c
      dimension rand(5),class(100),xk(101),xklass(100)
      i=o
      dseed=123457.d0
c
c       zero out the class array
c
      do 1 ll=1,101
      xk(ll)=0.0
    1 continue
c
c       fill in the class boundary array for water saturation
c
      class(1)=0.01
      do 2 ll=2,100
      lk=ll-1
      class(ll)=class(lk)+0.01
    2 continue
      xklass(1)=0.005
      do 3 ll=2,100
      kl=ll-1
      xklass(ll)=xklass(kl)+0.01
    3 continue
c
c       read in the parameters to be simulated
c
c       por,st,sww,shc,sm
      read(5,100) idpor,porh,porm,porl
      read(5,100) idrt,rth,rtm,rtl
      read(5,100) idrw,rwh,rwm,rwl
      read(5,100) idxn,xnh,xnm,xnl
      read(5,100) idxm,xmh,xmm,xml
      read(5,101) icount
c
c       this portion of the program generates the trail values for
c       each pass through the archie equation.  this portion is done
c       icount times
c
   10 if(i.eq.icount) go to 900
      call ggubs(dseed,5,rand)
      if (idrt.eq.0) go to 11
      call tri(rth,rtm,rtl,rand(1),rt)
      go to 12
   11 rt=rtl+rand(1)*(rth-rtl)
   12 if (idrw.eq.0) go to 21
      call tri(rwh,rwm,rwl,rand(2),rw)
      go to 22
   21 rw=rwl+rand(2)*(rwh-rwl)
   22 if (idxn.eq.0) go to 31
      call tri(xnh,xnm,xnl,rand(3),xn)
      go to 32
   31 xn=xnl+rand(3)*(xnh-xnl)
   32 if (idxm.eq.0) go to 41
      call tri(xmh,xmm,xml,rand(4),xm)
      go to 42
   41 xm=xml+rand(4)*(xmh-xml)
```

```
   42 if (idpor.eq.0) go to 51
       call tri(porh,porm,porl,rand(5),por)
       go to 52
   51 por=porl+rand(5)*(porh-porl)
c
c        calculate the water saturation with the data just generated
c        and determine the residual oil saturation.
c
   52 sw=(rt-xm+por*(xm-xn))/(por*(rw-xn))
      ros=1.0-sw
c
c        tally each ros into the class count array
c
      do 65 j=1,100
      jk=j
      if (ros-class(j)) 66,65,65
   65 continue
      jk=jk+1
   66 xk(jk)=xk(jk)+1
      i=i+1
      go to 10
  100 format(i5,3f10.3)
  101 format(i10)
c
c        calculate the statistics when the simulation is done
c
  900 xncnt=0.0
      sum=0.0
      xbar=0.0
      sumf=0.0
      sumf2=0.0
      s1=0.0
      s2=0.0
      sd=0.0
c        find n the sum of the frequencies
      do 950 j=1,100
      xncnt=xncnt+xk(j)
  950 continue
c        find the average saturation
      do 960 j=1,100
      sum=sum+(xk(j)*xklass(j))
  960 continue
      xbar=sum/xncnt
c        find the variance in the saturation
      do 970 j=1,100
      sumf=sumf+(xk(j)*xklass(j)**2)
      sumf2=sumf2+(xk(j)*xklass(j))**2
  970 continue
      s1=(sumf+(sumf2/xncnt))
      s2=s1/(xncnt-1.)
      sd=sqrt(s2)
      sdt=sd/sqrt(xncnt)
      t90=1.645*sdt
      t95=1.96*sdt
      t99=2.576*sdt
      c90u=xbar+t90
      c90l=xbar-t90
      c95u=xbar+t95
      c95l=xbar-t95
      c99u=xbar+t99
      c99l=xbar-t99
c
c        print out the run summary
c
      write(6,103)
      write(6,104)
  103 format(1h1,////,28x,'monte carlo simulation',/,35x,'of the',/,
     * 26x,'pulsed neutron equation'/)
  104 format(/,12x,'parameter',11x,'distribution',4x,'range of values',
     */,35x,'type *',5x,'high',2x,'average',3x,'low',/)
```

```
      write(6,105) idpor,porh,porm,porl
      write(6,106) idrt,rth,rtm,rtl
      write(6,107) idrw,rwh,rwm,rwl
      write(6,108) idxn,xnh,xnm,xnl
      write(6,109) idxm,xmh,xmm,xml
  105 format(/,12x,'porosity',15x,i5,5x,f6.3,2x,f6.3,1x,f6.3)
  106 format(/,12x,'sigma-bulk',13x,i5,5x,f6.3,2x,f6.3,1x,f6.3)
  107 format(/,12x,'sigma-water',12x,i5,5x,f6.3,2x,f6.3,1x,f6.3)
  108 format(/,12x,'sigma-hydrocarbon',6x,i5,5x,f6.3,2x,f6.3,1x,f6.3)
  109 format(/,12x,'sigma-matrix',11x,i5,5x,f6.3,2x,f6.3,1x,f6.3)
      write(6,120)
  120 format(//,12x,'* 0=uniform, 1=triangular')
      write(6,130) i,xncnt,xbar,s2,sd,c90l,c90u,c95l,c95u,c99l,c99u
  130 format(//,12x,'summary statistics based on',2x,i8,' trials',//,
     *12x,'number of observations',5x,f10.1,/,12x,'average saturation',
     *9x,f10.4,/,12x,'variance',19x,f10.4,/,12x,'standard deviation',
     *9x,f10.4,/,12x,'confidence interval at 90%',1x,f10.4,1x,f10.4,
     */,12x,'confidence interval at 95%',1x,f10.4,1x,f10.4,/,
     *12x,'confidence interval at 99%',1x,f10.4,1x,f10.4,//)
      write(6,140)
  140 format(1h1,////,27x,'summary of observations',/,13x,'mid-point',
     *7x,'frequency',6x,'relative',6x,'cumulative',/,44x,'frequency',
     *5x,'frequency',/)
      do 980 j=1,100
      if (xk(j).le.0.001) go to 980
      xkj=xk(j)/xncnt
      sumxkj=sumxkj+xkj
      write(6,141) xklass(j),xk(j),xkj,sumxkj
  980 continue
  141 format(1x,11x,f10.3,6x,f10.1,5x,f10.5,5x,f10.5)
  999 stop
      end
      subroutine tri(a,b,c,d,e)
      if (d-((b-c)/(a-c))) 10,20,20
   10 e=c+sqrt((b-c)*(a-c)*d)
      return
   20 e=a-sqrt((a-b)*(a-c)*(1.-d))
      return
      end
//go.sysin dd *
     1       0.31        0.29        0.27
     1      29.06        28.3       27.54
     1       89.0        87.0        85.0
     1       21.0        20.5        20.0
     1      14.55        11.9        9.25
      20000
     0       0.29        0.29        0.29
     0       21.6        21.6        21.6
     0       87.0        87.0        87.0
     0       20.5        20.5        20.5
     0       11.9        11.9        11.9
//
/*eof
```

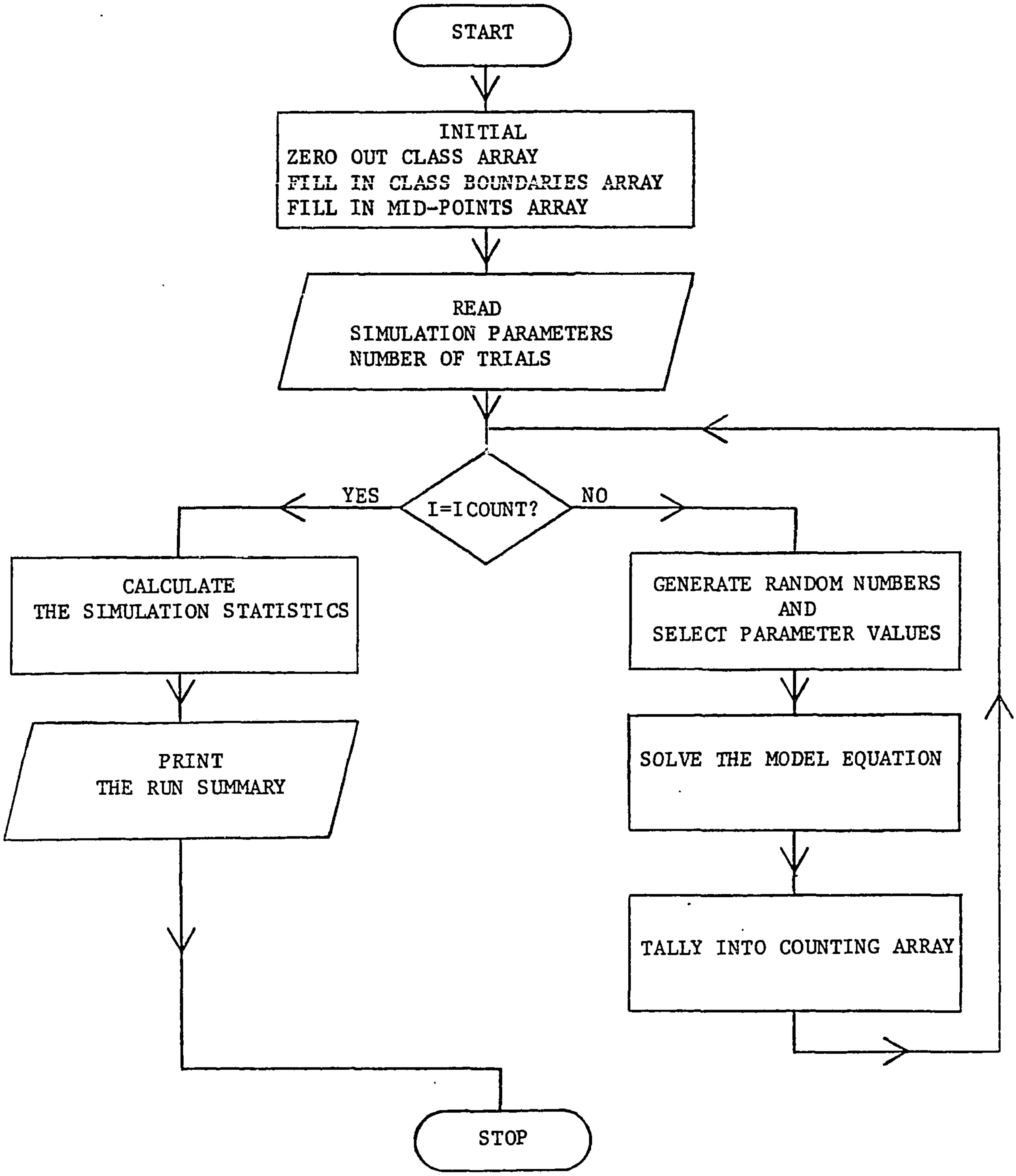

FIGURE VII. Monte Carlo Model Flowchart

APPENDIX B

TABLE XI

ZONE A CONVENTIONAL PULSED NEUTRON BEST CASE

MONTE CARLO SIMULATION
OF THE
PULSED NEUTRON EQUATION

PARAMETER	DISTRIBUTION TYPE #	RANGE OF VALUES HIGH	AVERAGE	LOW
POROSITY	1	0.310	0.[illegible]0	0.270
SIGMA-[illegible]	1	[illegible]	21.[illegible]	19.[illegible]
SIGMA-WATER	1	[illegible]	[illegible]	65.000
SIGMA-HYDROCARBON	1	21.000	[illegible]	20.000
SIGMA-MATRIX	1	[illegible]	11.900	3.711

0=NORMAL, 1=TRIANGULAR

SUMMARY STATISTICS BASED ON 20000 TRIALS

NUMBER OF OBSERVATIONS	20000.0
AVERAGE SATURATION	0.[illegible]
VARIANCE	0.0169
STANDARD DEVIATION	0.1300

SUMMARY OF OBSERVATIONS

MID-POINT	FREQUENCY	RELATIVE FREQUENCY	CUMULATIVE FREQUENCY
[illegible]	1.0	[illegible]	[illegible]
[illegible]	3.0	[illegible]	[illegible]
[illegible]	[illegible]	[illegible]	[illegible]
[illegible]	[illegible]	[illegible]	[illegible]
[illegible]	8.0	[illegible]	[illegible]
0.275	4.0	[illegible]	0.00115
[illegible]	[illegible]	[illegible]	[illegible]
[illegible]	14.0	[illegible]	[illegible]
[illegible]	[illegible]	[illegible]	[illegible]
[illegible]	31.0	[illegible]	[illegible]
[illegible]	47.0	[illegible]	[illegible]
[illegible]	57.0	[illegible]	[illegible]
0.345	71.0	[illegible]	[illegible]
[illegible]	[illegible]	[illegible]410	[illegible]
0.365	[illegible]	[illegible]	[illegible]
0.375	[illegible]	[illegible]	[illegible]
[illegible]	[illegible]	[illegible]	[illegible]
[illegible]	[illegible]	[illegible]	[illegible]
0.405	[illegible]	[illegible]	[illegible]
0.415	[illegible]	[illegible]	[illegible]
[illegible]	214.0	0.01070	[illegible]
0.435	[illegible]	[illegible]	[illegible]
0.445	[illegible]	0.01230	0.09410
[illegible]	[illegible]	[illegible]	[illegible]
[illegible]	[illegible]	[illegible]	[illegible]
[illegible]	[illegible]	[illegible]	[illegible]
[illegible]	[illegible]	0.01[illegible]0	[illegible]
[illegible]	[illegible]	[illegible]	[illegible]40
[illegible]	41[illegible]	[illegible]	[illegible]
[illegible]	431.0	[illegible]	[illegible]
[illegible]	461.0	[illegible]	[illegible]
[illegible]	463.0	[illegible]	[illegible]
0.545	[illegible]	0.02[illegible]	[illegible]
[illegible]	512.0	[illegible]	[illegible]
[illegible]	[illegible]	[illegible]	[illegible]
0.575	[illegible]	[illegible]	[illegible]
[illegible]	[illegible]	[illegible]	[illegible]
[illegible]	[illegible]	[illegible]	[illegible]
0.605	574.0	[illegible]	[illegible]
0.615	[illegible]	[illegible]	[illegible]
[illegible]	[illegible]	[illegible]	[illegible]
0.635	[illegible]	[illegible]	[illegible]
0.645	[illegible]	[illegible]	[illegible]
[illegible]	[illegible]	[illegible]	[illegible]
0.665	[illegible]	[illegible]910	[illegible]
0.675	[illegible]	[illegible]	[illegible]
[illegible]	[illegible]	[illegible]	[illegible]
0.695	543.0	0.02715	[illegible]
0.705	513.0	[illegible]	[illegible]
0.715	[illegible]	0.02400	[illegible]
[illegible]	431.0	[illegible]	[illegible]
0.735	[illegible]	[illegible]	[illegible]
[illegible]	[illegible]	0.01970	[illegible]
[illegible]	[illegible]	0.01960	[illegible]
0.765	[illegible]	0.01760	[illegible]
0.775	364.0	[illegible]	[illegible]
[illegible]	316.0	[illegible]	[illegible]
[illegible]	[illegible]	[illegible]	0.90110
[illegible]	[illegible]	0.01405	[illegible]
[illegible]	[illegible]	[illegible]	[illegible]
[illegible]	[illegible]	0.01175	0.93945
[illegible]	199.0	[illegible]	[illegible]
[illegible]	[illegible]	[illegible]	[illegible]
[illegible]	171.0	[illegible]	[illegible]
[illegible]	144.0	[illegible]	0.97445
[illegible]	114.0	[illegible]	[illegible]
[illegible]	[illegible]	[illegible]	[illegible]
[illegible]	76.0	[illegible]	[illegible]
0.905	[illegible]	[illegible]	[illegible]
0.915	[illegible]	[illegible]	[illegible]
[illegible]	32.0	[illegible]	[illegible]
[illegible]	[illegible]	[illegible]	[illegible]
[illegible]	[illegible]	[illegible]	[illegible]
[illegible]	[illegible]	[illegible]	[illegible]
0.965	11.0	[illegible]	[illegible]
0.975	1.0	[illegible]	[illegible]
[illegible]	1.0	[illegible]	1.[illegible]

TABLE XII

ZONE A CONVENTIONAL PULSED NEUTRON WORST CASE

[illegible]

PARAMETER	DISTRIBUTION TYPE #	RANGE OF VALUES HIGH	[illegible]	LOW
POROSITY	0	0.310	[illegible]	[illegible]
SIGMA-[illegible]	0	[illegible]	[illegible]	[illegible]
SIGMA-WATER	0	[illegible]	[illegible]	[illegible]
SIGMA-HYDROCARBON	0	[illegible]	[illegible]	20.000
SIGMA-MATRIX	0	[illegible]	11.900	[illegible]

[illegible]

SUMMARY STATISTICS BASED ON [illegible] TRIALS

NUMBER OF OBSERVATIONS	[illegible]
AVERAGE SATURATION	[illegible]
VARIANCE	[illegible]
STANDARD DEVIATION	[illegible]

SUMMARY OF OBSERVATIONS

MID-POINT	FREQUENCY *	RELATIVE FREQUENCY	CUMULATIVE FREQUENCY
0.155	2.0	0.00010	0.00010
0.165	2.0	0.00010	[illegible]
0.175	2.0	0.00010	[illegible]
0.185	7.0	[illegible]	[illegible]
0.195	12.0	[illegible]	[illegible]
0.205	21.0	[illegible]	[illegible]
0.215	13.0	[illegible]	[illegible]
0.225	21.0	[illegible]	[illegible]
0.235	49.0	[illegible]	[illegible]
0.245	38.0	0.00190	[illegible]
0.255	62.0	0.00311	[illegible]
0.265	75.0	[illegible]	[illegible]
0.275	85.0	[illegible]	[illegible]
0.285	76.0	[illegible]	[illegible]
0.295	93.0	[illegible]	[illegible]
0.305	123.0	[illegible]	[illegible]
0.315	144.0	[illegible]	[illegible]
0.325	152.0	[illegible]	[illegible]
0.335	196.0	[illegible]	[illegible]
0.345	197.0	[illegible]	[illegible]
0.355	197.0	[illegible]	[illegible]
0.365	222.0	0.01117	[illegible]
0.375	264.0	[illegible]	[illegible]
0.385	265.0	[illegible]	0.11416
0.395	240.0	0.01203	[illegible]
0.405	292.0	0.01463	[illegible]
0.415	276.0	[illegible]	[illegible]
0.425	309.0	0.01548	[illegible]
0.435	342.0	0.01714	[illegible]
0.445	303.0	[illegible]	[illegible]
0.455	307.0	[illegible]	[illegible]
0.465	334.0	[illegible]	[illegible]
0.475	[illegible]	0.01694	[illegible]
0.485	[illegible]	0.01614	[illegible]
0.495	317.0	[illegible]	[illegible]
0.505	330.0	[illegible]	[illegible]
0.515	349.0	0.01744	[illegible]
0.525	[illegible]	0.01774	[illegible]
0.535	[illegible]	[illegible]	[illegible]
0.545	[illegible]	[illegible]	[illegible]
0.555	[illegible]	[illegible]	[illegible]
0.565	[illegible]	[illegible]	[illegible]
0.575	[illegible]	[illegible]	[illegible]
0.585	[illegible]	0.01578	[illegible]
0.595	[illegible]	[illegible]	[illegible]
0.605	293.0	0.01458	[illegible]
0.615	[illegible]	[illegible]	[illegible]
0.625	340.0	0.01704	[illegible]
0.635	376.0	[illegible]	[illegible]
0.645	[illegible]	0.01619	[illegible]
0.655	334.0	0.01674	[illegible]
0.665	[illegible]	[illegible]	0.56735
0.675	[illegible]	[illegible]	[illegible]
0.685	[illegible]	[illegible]	[illegible]
0.695	336.0	[illegible]	[illegible]
0.705	310.0	[illegible]	0.63475
0.715	342.0	0.01714	[illegible]
0.725	296.0	[illegible]	[illegible]
0.735	328.0	0.01644	0.66315
0.745	358.0	0.01794	0.70109
0.755	392.0	0.01964	0.72073
0.765	314.0	0.01573	0.73647
0.775	350.0	0.01754	0.75401
0.785	333.0	0.01669	0.77069
0.795	330.0	0.01654	0.78723
0.805	336.0	0.01684	[illegible]
0.815	337.0	0.01689	[illegible]
0.825	318.0	0.01594	0.83689
0.835	332.0	0.01664	0.85353
0.845	341.0	0.01709	0.87061
0.855	310.0	[illegible]	[illegible]
0.865	266.0	0.01333	[illegible]
0.875	267.0	0.01338	[illegible]
0.885	227.0	0.01138	0.92463
0.895	255.0	0.01278	0.93741
0.905	194.0	0.00972	0.94713
0.915	203.0	0.01017	0.95730
0.925	161.0	0.00807	0.96537
0.935	136.0	0.00681	0.97219
0.945	156.0	[illegible]	0.98000
0.955	121.0	[illegible]	[illegible]
0.965	82.0	0.00411	0.99018
0.975	79.0	[illegible]	0.99414
0.985	73.0	0.00366	[illegible]
0.995	44.0	[illegible]	1.00000

TABLE XIII

ZONE B CONVENTIONAL PULSED NEUTRON BEST CASE

MONTE CARLO SIMULATION
OF THE
[illegible] EQUATION

PARAMETER	DISTRIBUTION TYPE *	RANGE OF VALUES HIGH	AVERAGE	LOW
POROSITY	1	0.310	0.290	0.270
SIGMA-BULK	1	30.640	28.300	25.952
SIGMA-WATER	1	87.000	87.000	85.600
SIGMA HYDROCARBON	1	21.000	20.500	20.000
SIGMA-MATRIX	1	20.009	11.900	3.711

* 0=UNIFORM, 1=TRIANGULAR

SUMMARY STATISTICS BASED ON 20000 TRIALS

NUMBER OF OBSERVATIONS	20000.0
AVERAGE SATURATION	0.2798
VARIANCE	0.0179
STANDARD DEVIATION	0.1340

SUMMARY OF OBSERVATIONS

MID-POINT	FREQUENCY	RELATIVE FREQUENCY	CUMULATIVE FREQUENCY
0.0	396.0	0.01980	0.01980
0.005	83.0	0.00415	0.02395
0.015	88.0	0.00440	0.02835
0.025	117.0	0.00585	0.03420
0.035	126.0	0.00630	0.04050
0.045	144.0	0.00720	0.04770
0.055	175.0	0.00875	0.05645
0.065	185.0	0.00925	0.06570
0.075	211.0	0.01055	0.07625
0.085	259.0	0.01295	0.08920
0.095	254.0	0.01270	0.10190
0.105	269.0	0.01345	0.11535
0.115	279.0	0.01395	0.12930
0.125	299.0	0.01495	0.14425
0.135	331.0	0.01655	0.16080
0.145	343.0	0.01715	0.17795
0.155	425.0	0.02125	0.19920
0.165	374.0	0.01870	0.21790
0.175	413.0	0.02065	0.23855
0.185	465.0	0.02325	0.26180
0.195	462.0	0.02310	0.28490
0.205	488.0	0.02440	0.30930
0.215	528.0	0.02640	0.33570
0.225	516.0	0.02580	0.36150
0.235	528.0	0.02640	0.38790
0.245	560.0	0.02800	0.41590
0.255	581.0	0.02905	0.44495
0.265	528.0	0.02640	0.47135
0.275	529.0	0.02645	0.49780
0.285	562.0	0.02810	0.52590
0.295	577.0	0.02885	0.55475
0.305	564.0	0.02820	0.58295
0.315	521.0	0.02605	0.60900
0.325	544.0	0.02720	0.63620
0.335	514.0	0.02570	0.66190
0.345	503.0	0.02515	0.68705
0.355	490.0	0.02450	0.71155
0.365	525.0	0.02625	0.73780
0.375	460.0	0.02300	0.76080
0.385	444.0	0.02220	0.78300
0.395	422.0	0.02110	0.80410
0.405	391.0	0.01955	0.82365
0.415	357.0	0.01785	0.84150
0.425	335.0	0.01675	0.85825
0.435	340.0	0.01700	0.87525
0.445	285.0	0.01425	0.88950
0.455	285.0	0.01425	0.90375
0.465	260.0	0.01300	0.91675
0.475	246.0	0.01230	0.92905
0.485	231.0	0.01155	0.94060
0.495	186.0	0.00930	0.94990
0.505	157.0	0.00785	0.95775
0.515	148.0	0.00740	0.96515
0.525	141.0	0.00705	0.97220
0.535	113.0	0.00565	0.97785
0.545	100.0	0.00500	0.98285
0.555	66.0	0.00330	0.98615
0.565	68.0	0.00340	0.98955
0.575	50.0	0.00250	0.99205
0.585	49.0	0.00245	0.99450
0.595	33.0	0.00165	0.99615
0.605	15.0	0.00075	0.99690
0.615	21.0	0.00105	0.99795
0.625	14.0	0.00070	0.99865
0.635	16.0	0.00080	0.99945
0.645	9.0	0.00045	0.99990
0.665	1.0	0.00005	0.99995
0.675	1.0	0.00005	1.00000

TABLE XIV

ZONE B CONVENTIONAL PULSED NEUTRON WORST CASE

MONTE CARLO SIMULATION
OF THE
PULSED NEUTRON EQUATION

PARAMETER	DISTRIBUTION TYPE *	RANGE OF VALUES HIGH	AVERAGE	LOW
POROSITY	0	0.310	0.290	0.270
SIGMA-BULK	0	30.640	28.300	25.952
SIGMA-WATER	0	59.000	57.000	55.000
SIGMA-HYDROCARBON	0	21.000	20.500	20.000
SIGMA-MATRIX	0	20.009	11.860	3.711

* 0-UNIFORM, 1-TRIANGULAR

SUMMARY STATISTICS BASED ON 20000 TRIALS

NUMBER OF OBSERVATIONS	20000.0
AVERAGE SATURATION	0.2837
VARIANCE	0.0336
STANDARD DEVIATION	0.1834

SUMMARY OF OBSERVATIONS

MID-POINT	FREQUENCY	RELATIVE FREQUENCY	CUMULATIVE FREQUENCY
0.0	1610.0	0.08050	0.08050
0.005	185.0	0.00925	0.08975
0.015	210.0	0.01050	0.10025
0.025	204.0	0.01020	0.11045
0.035	197.0	0.00985	0.12030
0.045	275.0	0.01375	0.13405
0.055	272.0	0.01360	0.14765
0.065	254.0	0.01270	0.16035
0.075	273.0	0.01365	0.17400
0.085	295.0	0.01475	0.18875
0.095	290.0	0.01450	0.20325
0.105	312.0	0.01560	0.21885
0.115	304.0	0.01520	0.23405
0.125	299.0	0.01495	0.24900
0.135	316.0	0.01580	0.26480
0.145	342.0	0.01710	0.28190
0.155	321.0	0.01605	0.29795
0.165	335.0	0.01675	0.31470
0.175	337.0	0.01685	0.33155
0.185	364.0	0.01820	0.34975
0.195	312.0	0.01560	0.36535
0.205	329.0	0.01645	0.38180
0.215	347.0	0.01735	0.39915
0.225	317.0	0.01585	0.41500
0.235	387.0	0.01935	0.43435
0.245	306.0	0.01530	0.44965
0.255	323.0	0.01615	0.46580
0.265	329.0	0.01645	0.48225
0.275	318.0	0.01590	0.49815
0.285	311.0	0.01555	0.51370
0.295	319.0	0.01595	0.52965
0.305	335.0	0.01675	0.54640
0.315	326.0	0.01630	0.56270
0.325	338.0	0.01690	0.57960
0.335	333.0	0.01665	0.59625
0.345	314.0	0.01570	0.61195
0.355	342.0	0.01710	0.62905
0.365	296.0	0.01480	0.64385
0.375	336.0	0.01680	0.66065
0.385	342.0	0.01710	0.67775
0.395	353.0	0.01765	0.69540
0.405	351.0	0.01755	0.71295
0.415	353.0	0.01765	0.73060
0.425	357.0	0.01785	0.74845
0.435	351.0	0.01755	0.76600
0.445	339.0	0.01695	0.78295
0.455	332.0	0.01660	0.79955
0.465	292.0	0.01460	0.81415
0.475	294.0	0.01470	0.82885
0.485	288.0	0.01440	0.84325
0.495	299.0	0.01495	0.85820
0.505	250.0	0.01250	0.87070
0.515	242.0	0.01210	0.88280
0.525	248.0	0.01240	0.89520
0.535	255.0	0.01275	0.90795
0.545	211.0	0.01055	0.91850
0.555	217.0	0.01085	0.92935
0.565	185.0	0.00925	0.93860
0.575	177.0	0.00885	0.94745
0.585	164.0	0.00820	0.95565
0.595	152.0	0.00760	0.96325
0.605	117.0	0.00585	0.96910
0.615	127.0	0.00635	0.97545
0.625	112.0	0.00560	0.98105
0.635	94.0	0.00470	0.98575
0.645	69.0	0.00345	0.98920
0.655	69.0	0.00345	0.99265
0.665	49.0	0.00245	0.99510
0.675	43.0	0.00215	0.99725
0.685	27.0	0.00135	0.99860
0.695	19.0	0.00095	0.99955
0.705	6.0	0.00030	0.99985
0.715	3.0	0.00015	1.00000

TABLE XV

WATERFLOOD LOG-INJECT-LOG ZONE 1 BEST CASE

[illegible]

PARAMETER	DISTRIBUTION TYPE *	RANGE OF VALUES HIGH	AVERAGE	LOW
POROSITY	1	0.260	0.250	0.240
SIGMA-BULK 1	1	18.415	17.[illegible]	17.229
SIGMA-BULK 2	1	32.406	[illegible]	26.664
SIGMA-WATER 1	1	42.925	[illegible]	42.0[illegible]
SIGMA-WATER 2	1	100.495	99.500	[illegible]

* 0=UNIFORM, 1=TRIANGULAR

SUMMARY STATISTICS BASED ON 20000 TRIALS

NUMBER OF OBSERVATIONS	20000.0
AVERAGE SATURATION	0.1770
VARIANCE	0.0072
STANDARD DEVIATION	0.0847

SUMMARY OF OBSERVATIONS

MID-POINT	FREQUENCY	RELATIVE FREQUENCY	CUMULATIVE FREQUENCY
0.0	287.0	0.01435	0.01435
0.005	147.0	0.00735	0.02170
0.015	190.0	0.00950	0.03120
0.025	245.0	0.01225	0.04345
0.035	298.0	0.01490	0.05835
0.045	376.0	0.01880	0.07715
0.055	348.0	0.01740	0.09455
0.065	[illegible]	0.02270	0.11725
0.075	473.0	0.02365	0.14110
0.085	530.0	0.02650	0.16760
0.095	625.0	0.03125	0.19885
0.105	614.0	[illegible]	[illegible]
0.115	654.0	[illegible]	[illegible]
0.125	723.0	0.03640	[illegible]
0.135	750.0	0.03750	[illegible]
0.145	862.0	0.04310	[illegible]
0.155	873.0	0.04365	[illegible]
0.165	880.0	0.04400	[illegible]
0.175	927.0	0.04635	[illegible]
0.185	909.0	0.04545	[illegible]
0.195	905.0	0.04525	[illegible]
0.205	839.0	0.04195	[illegible]
0.215	799.0	0.03995	[illegible]
0.225	788.0	0.03940	[illegible]
0.235	716.0	0.03580	0.76115
0.245	666.0	[illegible]	[illegible]
0.255	590.0	0.02950	[illegible]
0.265	564.0	0.02820	[illegible]
0.275	483.0	0.02415	[illegible]
0.285	439.0	0.02195	[illegible]
0.295	400.0	0.02000	0.91825
0.305	365.0	0.01825	[illegible]
0.315	294.0	0.01470	0.95120
0.325	271.0	0.01355	0.96475
0.335	212.0	0.01060	0.97535
0.345	171.0	0.00855	0.98390
0.355	131.0	0.00655	0.99045
0.365	88.0	0.00440	0.99485
0.375	41.0	0.00205	0.99690
0.385	31.0	0.00155	0.99845
0.395	21.0	0.00105	0.99950
0.405	9.0	0.00045	0.99995
0.435	1.0	0.00005	1.00000

TABLE XVI

WATERFLOOD LOG-INJECT-LOG ZONE 1 WORST CASE

MONTE CARLO SIMULATION
IN THE
WATERFLOOD LIL

PARAMETER	DISTRIBUTION TYPE *	RANGE OF VALUES HIGH	AVERAGE	LOW
POROSITY	0	0.260	0.200	0.140
SIGMA-BULK 1	0	[illegible]	[illegible]	[illegible]
SIGMA-BULK 2	0	32.406	29.535	26.664
SIGMA-WATER 1	0	42.925	42.500	42.075
SIGMA-WATER 2	0	100.495	99.500	98.505

* 0=UNIFORM, 1=TRIANGULAR

SUMMARY STATISTICS BASED ON 20000 TRIALS

NUMBER OF OBSERVATIONS	20000.0
AVERAGE SATURATION	[illegible]
VARIANCE	0.0137
STANDARD DEVIATION	0.1171

SUMMARY OF OBSERVATIONS

MID-POINT	FREQUENCY	RELATIVE FREQUENCY	CUMULATIVE FREQUENCY
0.0	1484.0	0.07420	0.07420
0.005	[illegible]	[illegible]	[illegible]
0.015	[illegible]	[illegible]	[illegible]
0.025	423.0	0.02115	[illegible]
0.035	[illegible]	[illegible]	[illegible]
0.045	[illegible]	[illegible]	[illegible]
0.055	[illegible]	0.02525	[illegible]
0.065	[illegible]	[illegible]	[illegible]
0.075	470.0	[illegible]	[illegible]
0.085	[illegible]	0.02425	[illegible]
0.095	[illegible]	0.02430	[illegible]
0.105	504.0	[illegible]	[illegible]
0.115	483.0	0.02415	[illegible]
0.125	514.0	[illegible]	[illegible]
0.135	[illegible]	[illegible]	[illegible]
0.145	[illegible]	[illegible]	[illegible]
0.155	512.0	[illegible]	[illegible]
0.165	521.0	[illegible]	[illegible]
0.175	[illegible]	[illegible]	[illegible]
0.185	475.0	[illegible]	[illegible]
0.195	509.0	0.02545	[illegible]
0.205	[illegible]	[illegible]	[illegible]
0.215	518.0	0.02590	[illegible]
0.225	524.0	0.02620	[illegible]
0.235	470.0	0.02350	0.66010
0.245	493.0	0.02465	[illegible]
0.255	494.0	0.02470	0.70945
0.265	499.0	0.02495	0.73440
0.275	508.0	0.02540	[illegible]
0.285	517.0	0.02585	[illegible]
0.295	453.0	0.02265	0.80830
0.305	[illegible]	[illegible]	0.83195
0.315	481.0	0.02405	0.85600
0.325	488.0	0.02440	0.88040
0.335	431.0	0.02155	0.90195
0.345	419.0	0.02095	[illegible]
0.355	364.0	0.01820	0.94110
0.365	351.0	0.01755	[illegible]
0.375	260.0	0.01300	0.97165
0.385	193.0	0.00965	0.98130
0.395	173.0	0.00865	[illegible]
0.405	97.0	0.00485	[illegible]
0.415	61.0	0.00305	[illegible]
0.425	[illegible]	0.00145	[illegible]
0.435	11.0	[illegible]	[illegible]
0.445	2.0	0.00010	[illegible]
0.455	1.0	0.00005	1.00000

TABLE XVII

WATERFLOOD LOG-INJECT-LOG ZONE 2 BEST CASE

MONTE CARLO SIMULATION
OF THE
WATERFLOOD LIL

PARAMETER	DISTRIBUTION TYPE *	RANGE OF VALUES HIGH	AVERAGE	LOW
POROSITY	1	[illegible]	0.270	[illegible]
SIGMA-BULK 1	1	19.473	[illegible]	[illegible]
SIGMA-BULK 2	1	36.392	33.204	[illegible]
SIGMA-WATER 1	1	42.925	42.500	42.075
SIGMA-WATER 2	1	100.495	99.500	98.505

* 0=UNIFORM, 1=TRIANGULAR

SUMMARY STATISTICS BASED ON 20000 TRIALS

NUMBER OF OBSERVATIONS	20000.0
AVERAGE SATURATION	0.1360
VARIANCE	0.0103
STANDARD DEVIATION	0.1017

SUMMARY OF OBSERVATIONS

MID-POINT	FREQUENCY	RELATIVE FREQUENCY	CUMULATIVE FREQUENCY
0.0	2824.0	0.14120	0.14120
0.005	394.0	0.01970	[illegible]
0.015	453.0	0.02265	[illegible]
0.025	463.0	[illegible]	[illegible]
0.035	470.0	0.02350	[illegible]
0.045	494.0	0.02470	[illegible]
0.055	529.0	[illegible]	[illegible]
0.065	541.0	[illegible]	[illegible]
0.075	[illegible]	[illegible]	[illegible]
0.085	615.0	0.03075	[illegible]
0.095	656.0	0.03280	[illegible]
0.105	[illegible]	[illegible]	[illegible]
0.115	[illegible]	[illegible]	[illegible]
0.125	679.0	0.03395	[illegible]
0.135	684.0	0.03420	[illegible]
0.145	695.0	0.03475	0.57065
0.155	[illegible]	0.03440	[illegible]
0.165	642.0	0.03210	0.62715
0.175	627.0	0.03135	[illegible]
0.185	615.0	0.03075	[illegible]
0.195	584.0	0.02920	[illegible]
0.205	510.0	0.02550	0.75395
0.215	486.0	0.02430	0.77825
0.225	491.0	0.02455	[illegible]
0.235	440.0	0.02200	[illegible]
0.245	408.0	0.02040	[illegible]
0.255	385.0	0.01925	[illegible]
0.265	362.0	0.01810	[illegible]
0.275	329.0	0.01645	[illegible]
0.285	283.0	0.01415	0.91315
0.295	296.0	0.01480	[illegible]
0.305	248.0	0.01240	[illegible]
0.315	227.0	0.01145	0.95180
0.325	209.0	0.01045	0.96225
0.335	178.0	0.00890	0.97115
0.345	164.0	0.00820	0.97935
0.355	111.0	0.00555	0.98490
0.365	108.0	0.00540	0.99030
0.375	74.0	0.00370	0.99400
0.385	42.0	0.00210	0.99610
0.395	32.0	0.00160	0.99770
0.405	25.0	0.00125	0.99895
0.415	19.0	[illegible]	[illegible]
0.425	2.0	0.00010	[illegible]
0.455	1.0	0.00005	1.00000

TABLE XVIII

WATERFLOOD LOG-INJECT-LOG ZONE 2 WORST CASE

MONTE CARLO SIMULATION
OF THE
WATERFLOOD LIL

PARAMETER	DISTRIBUTION TYPE *	RANGE OF VALUES HIGH	AVERAGE	LOW
POROSITY	0	0.280	0.270	0.260
SIGMA-BULK 1	0	19.423	18.774	18.125
SIGMA-BULK 2	0	34.382	32.204	30.026
SIGMA-WATER 1	0	42.925	42.500	42.075
SIGMA-WATER 2	0	100.495	99.500	98.505

* 0=UNIFORM, 1=TRIANGULAR

SUMMARY STATISTICS BASED ON 20000 TRIALS

NUMBER OF OBSERVATIONS	20000.0
AVERAGE SATURATION	0.1489
VARIANCE	0.0179
STANDARD DEVIATION	0.1339

SUMMARY OF OBSERVATIONS

MID-POINT	FREQUENCY	RELATIVE FREQUENCY	CUMULATIVE FREQUENCY
0.0	5261.0	0.26305	0.26305
0.005	367.0	0.01835	0.28140
0.015	341.0	0.01705	0.29845
0.025	374.0	0.01870	0.31715
0.035	363.0	0.01815	0.33530
0.045	382.0	0.01910	0.35440
0.055	336.0	0.01680	0.37120
0.065	370.0	0.01850	0.38970
0.075	382.0	0.01910	0.40880
0.085	386.0	0.01930	0.42810
0.095	356.0	0.01780	0.44590
0.105	417.0	0.02085	0.46675
0.115	377.0	0.01885	0.48560
0.125	332.0	0.01660	0.50220
0.135	366.0	0.01830	0.52050
0.145	373.0	0.01865	0.53915
0.155	373.0	0.01865	0.55780
0.165	357.0	0.01785	0.57565
0.175	381.0	0.01905	0.59470
0.185	392.0	0.01960	0.61430
0.195	410.0	0.02050	0.63480
0.205	360.0	0.01800	0.65280
0.215	378.0	0.01890	0.67170
0.225	370.0	0.01850	0.69020
0.235	385.0	0.01925	0.70945
0.245	377.0	0.01885	0.72830
0.255	355.0	0.01775	0.74605
0.265	360.0	0.01800	0.76405
0.275	356.0	0.01780	0.78185
0.285	374.0	0.01870	0.80055
0.295	344.0	0.01720	0.81775
0.305	352.0	0.01760	0.83535
0.315	351.0	0.01755	0.85290
0.325	353.0	0.01765	0.87055
0.335	354.0	0.01770	0.88825
0.345	354.0	0.01770	0.90595
0.355	341.0	0.01705	0.92300
0.365	325.0	0.01625	0.93925
0.375	276.0	0.01380	0.95305
0.385	245.0	0.01225	0.96530
0.395	213.0	0.01065	0.97595
0.405	185.0	0.00925	0.98520
0.415	129.0	0.00645	0.99165
0.425	77.0	0.00385	0.99550
0.435	51.0	0.00255	0.99805
0.445	26.0	0.00130	0.99935
0.455	10.0	0.00050	0.99985
0.465	2.0	0.00010	0.99995
0.475	1.0	0.00005	1.00000

TABLE XIX

WATERFLOOD LOG-INJECT-LOG ZONE 3 BEST CASE

MONTE CARLO SIMULATION
OF THE
WATERFLOOD LIL

PARAMETER	DISTRIBUTION TYPE *	RANGE OF VALUES HIGH	AVERAGE	LOW
POROSITY	1	0.280	0.270	0.260
SIGMA MATRIX 1	1	19.491	18.824	18.151
SIGMA-MATRIX 2	1	36.397	42.277	35.647
SIGMA WATER 1	1	42.925	42.500	42.075
SIGMA-WATER 2	1	100.495	99.500	98.505

* 0=UNIFORM, 1=TRIANGULAR

SUMMARY STATISTICS BASED ON 20000 TRIALS

NUMBER OF OBSERVATIONS	20000.0
AVERAGE SATURATION	0.1349
VARIANCE	0.0103
STANDARD DEVIATION	0.1015

SUMMARY OF OBSERVATIONS

MID-POINT	FREQUENCY	RELATIVE FREQUENCY	CUMULATIVE FREQUENCY
0.0	2946.0	0.14730	0.14730
0.005	318.0	0.01590	0.16320
0.015	463.0	0.02315	0.18635
0.025	463.0	0.02315	0.20950
0.035	460.0	0.02300	0.23250
0.045	515.0	0.02575	0.25825
0.055	517.0	0.02585	0.28410
0.065	547.0	0.02735	0.31145
0.075	574.0	0.02870	0.34015
0.085	619.0	0.03095	0.37110
0.095	653.0	0.03265	0.40375
0.105	664.0	0.03320	0.43695
0.115	719.0	0.03595	0.47290
0.125	667.0	0.03335	0.50625
0.135	681.0	0.03405	0.54030
0.145	701.0	0.03505	0.57535
0.155	690.0	0.03450	0.60985
0.165	627.0	0.03135	0.64120
0.175	620.0	0.03100	0.67220
0.185	620.0	0.03100	0.70320
0.195	574.0	0.02870	0.73190
0.205	505.0	0.02525	0.75715
0.215	500.0	0.02500	0.78215
0.225	476.0	0.02380	0.80595
0.235	424.0	0.02120	0.82715
0.245	417.0	0.02085	0.84800
0.255	376.0	0.01880	0.86680
0.265	360.0	0.01800	0.88480
0.275	309.0	0.01545	0.90025
0.285	294.0	0.01470	0.91495
0.295	290.0	0.01450	0.92945
0.305	247.0	0.01235	0.94180
0.315	226.0	0.01130	0.95310
0.325	208.0	0.01040	0.96350
0.335	177.0	0.00885	0.97235
0.345	158.0	0.00790	0.98025
0.355	108.0	0.00540	0.98565
0.365	103.0	0.00515	0.99080
0.375	71.0	0.00355	0.99435
0.385	38.0	0.00190	0.99625
0.395	30.0	0.00150	0.99775
0.405	25.0	0.00125	0.99900
0.415	17.0	0.00085	0.99985
0.425	2.0	0.00010	0.99995
0.455	1.0	0.00005	1.00000

TABLE XX

WATERFLOOD LOG-INJECT-LOG ZONE 3 WORST CASE

MONTE CARLO SIMULATION
OF THE
WATERFLOOD LIL

PARAMETER	DISTRIBUTION TYPE *	RANGE OF VALUES HIGH	AVERAGE	LOW
POROSITY	0	0.300	0.270	0.240
SIGMA-BULK 1	0	19.451	18.804	18.151
SIGMA-BULK 2	0	26.397	23.222	20.047
SIGMA-WATER 1	0	42.925	42.500	42.075
SIGMA WATER 2	0	100.495	99.503	98.505

* 0=UNIFORM, 1=TRIANGULAR

SUMMARY STATISTICS BASED ON 20000 TRIALS

NUMBER OF OBSERVATIONS	20000.0
AVERAGE SATURATION	0.1470
VARIANCE	0.0178
STANDARD DEVIATION	0.1335

SUMMARY OF OBSERVATIONS

MID-POINT	FREQUENCY	RELATIVE FREQUENCY	CUMULATIVE FREQUENCY
0.0	5309.0	0.26545	0.26545
0.005	354.0	0.01770	0.28315
0.015	351.0	0.01755	0.30070
0.025	368.0	0.01840	0.31910
0.035	375.0	0.01875	0.33785
0.045	392.0	0.01960	0.35745
0.055	325.0	0.01625	0.37370
0.065	375.0	0.01875	0.39245
0.075	383.0	0.01915	0.41160
0.085	382.0	0.01910	0.43070
0.095	367.0	0.01835	0.44905
0.105	402.0	0.02010	0.46915
0.115	375.0	0.01875	0.48790
0.125	335.0	0.01675	0.50465
0.135	364.0	0.01820	0.52285
0.145	394.0	0.01970	0.54255
0.155	355.0	0.01775	0.56030
0.165	352.0	0.01760	0.57790
0.175	398.0	0.01990	0.59780
0.185	386.0	0.01930	0.61710
0.195	416.0	0.02080	0.63790
0.205	355.0	0.01775	0.65565
0.215	373.0	0.01865	0.67430
0.225	370.0	0.01850	0.69280
0.235	382.0	0.01910	0.71190
0.245	376.0	0.01880	0.73070
0.255	384.0	0.01920	0.74990
0.265	359.0	0.01795	0.76785
0.275	349.0	0.01745	0.78530
0.285	362.0	0.01810	0.80340
0.295	332.0	0.01660	0.82000
0.305	360.0	0.01800	0.83800
0.315	356.0	0.01780	0.85580
0.325	359.0	0.01795	0.87375
0.335	352.0	0.01760	0.89135
0.345	339.0	0.01695	0.90830
0.355	345.0	0.01725	0.92555
0.365	305.0	0.01525	0.94080
0.375	280.0	0.01400	0.95480
0.385	230.0	0.01150	0.96630
0.395	207.0	0.01035	0.97665
0.405	180.0	0.00900	0.98565
0.415	126.0	0.00630	0.99195
0.425	75.0	0.00375	0.99570
0.435	48.0	0.00240	0.99810
0.445	25.0	0.00125	0.99935
0.455	10.0	0.00050	0.99985
0.465	2.0	0.00010	0.99995
0.475	1.0	0.00005	1.00000

TABLE XXI

IMPROVED WATERFLOOD LOG-INJECT-LOG ZONE 1 BEST CASE

MONTE CARLO SIMULATION
OF THE
WATERFLOOD LIL

PARAMETER	DISTRIBUTION TYPE *	RANGE OF VALUES HIGH	AVERAGE	LOW
POROSITY	1	0.345	0.325	0.305
SIGMA-BULK 1	1	18.509	18.070	17.631
SIGMA-BULK 2	1	28.705	27.966	27.227
SIGMA-WATER 1	1	32.468	31.532	30.596
SIGMA-WATER 2	1	75.559	73.387	71.215

* 0=UNIFORM, 1=TRIANGULAR

SUMMARY STATISTICS BASED ON 20000 TRIALS

NUMBER OF OBSERVATIONS	20000.0
AVERAGE SATURATION	0.2715
VARIANCE	0.0013
STANDARD DEVIATION	0.0357

SUMMARY OF OBSERVATIONS

MID-POINT	FREQUENCY	RELATIVE FREQUENCY	CUMULATIVE FREQUENCY
0.135	1.0	0.00005	0.00005
0.145	4.0	0.00020	0.00025
0.155	10.0	0.00050	0.00075
0.165	27.0	0.00135	0.00210
0.175	66.0	0.00330	0.00540
0.185	129.0	0.00645	0.01185
0.195	244.0	0.01220	0.02405
0.205	425.0	0.02125	0.04530
0.215	683.0	0.03415	0.07945
0.225	962.0	0.04810	0.12755
0.235	1278.0	0.06390	0.19145
0.245	1605.0	0.08025	0.27170
0.255	1908.0	0.09540	0.36710
0.265	2164.0	0.10820	0.47530
0.275	2232.0	0.11160	0.58690
0.285	2109.0	0.10545	0.69235
0.295	1797.0	0.08985	0.78220
0.305	1514.0	0.07570	0.85790
0.315	1094.0	0.05470	0.91260
0.325	816.0	0.04080	0.95340
0.335	485.0	0.02425	0.97765
0.345	255.0	0.01275	0.99040
0.355	125.0	0.00625	0.99665
0.365	46.0	0.00230	0.99895
0.375	15.0	0.00075	0.99970
0.385	4.0	0.00020	0.99990
0.395	1.0	0.00005	0.99995
0.405	1.0	0.00005	1.00000

TABLE XXII

IMPROVED WATERFLOOD LOG-INJECT-LOG ZONE 1 WORST CASE

MONTE CARLO SIMULATION
OF THE
WATERFLOOD LIL

PARAMETER	DISTRIBUTION TYPE *	RANGE OF VALUES HIGH	AVERAGE	LOW
POROSITY	0	0.345	0.325	0.305
SIGMA-BULK 1	0	18.509	18.070	17.631
SIGMA-BULK 2	0	28.705	27.966	27.227
SIGMA-WATER 1	0	32.468	31.532	30.596
SIGMA-WATER 2	0	75.559	73.387	71.215

* 0=UNIFORM, 1=TRIANGULAR

SUMMARY STATISTICS BASED ON 20000 TRIALS

NUMBER OF OBSERVATIONS	20000.0
AVERAGE SATURATION	0.2706
VARIANCE	0.0026
STANDARD DEVIATION	0.0505

SUMMARY OF OBSERVATIONS

MID-POINT	FREQUENCY	RELATIVE FREQUENCY	CUMULATIVE FREQUENCY
0.105	5.0	0.00025	0.00025
0.115	7.0	0.00035	0.00060
0.125	26.0	0.00130	0.00190
0.135	49.0	0.00245	0.00435
0.145	93.0	0.00465	0.00900
0.155	123.0	0.00615	0.01515
0.165	198.0	0.00990	0.02505
0.175	287.0	0.01435	0.03940
0.185	424.0	0.02120	0.06060
0.195	563.0	0.02815	0.08875
0.205	687.0	0.03435	0.12310
0.215	871.0	0.04355	0.16665
0.225	968.0	0.04840	0.21505
0.235	1144.0	0.05720	0.27225
0.245	1349.0	0.06745	0.33970
0.255	1431.0	0.07155	0.41125
0.265	1463.0	0.07315	0.48440
0.275	1569.0	0.07845	0.56285
0.285	1447.0	0.07235	0.63520
0.295	1419.0	0.07095	0.70615
0.305	1293.0	0.06465	0.77080
0.315	1162.0	0.05810	0.82890
0.325	941.0	0.04705	0.87595
0.335	800.0	0.04000	0.91595
0.345	592.0	0.02960	0.94555
0.355	442.0	0.02210	0.96765
0.365	308.0	0.01540	0.98305
0.375	165.0	0.00825	0.99130
0.385	110.0	0.00550	0.99680
0.395	42.0	0.00210	0.99890
0.405	15.0	0.00075	0.99965
0.415	6.0	0.00030	0.99995
0.425	1.0	0.00005	1.00000

TABLE XXIII

IMPROVED WATERFLOOD LOG-INJECT-LOG ZONE 2 BEST CASE

MONTE CARLO SIMULATION
OF THE
WATERFLOOD LIL

PARAMETER	DISTRIBUTION TYPE *	RANGE OF VALUES HIGH	AVERAGE	LOW
POROSITY	1	0.345	0.325	0.305
SIGMA-BULK 1	1	17.523	16.908	16.293
SIGMA-BULK 2	1	27.356	26.639	25.922
SIGMA-WATER 1	1	32.460	31.522	30.596
SIGMA-WATER 2	1	75.559	73.307	71.215

* 0=UNIFORM, 1=TRIANGULAR

SUMMARY STATISTICS BASED ON 20000 TRIALS

NUMBER OF OBSERVATIONS	20000.0
AVERAGE SATURATION	0.2836
VARIANCE	0.0014
STANDARD DEVIATION	0.0373

SUMMARY OF OBSERVATIONS

MID-POINT	FREQUENCY	RELATIVE FREQUENCY	CUMULATIVE FREQUENCY
0.145	1.0	0.00005	0.00005
0.155	8.0	0.00040	0.00045
0.165	10.0	0.00050	0.00095
0.175	40.0	0.00200	0.00295
0.185	73.0	0.00365	0.00660
0.195	133.0	0.00665	0.01325
0.205	250.0	0.01250	0.02575
0.215	405.0	0.02025	0.04600
0.225	669.0	0.03345	0.07945
0.235	932.0	0.04660	0.12605
0.245	1200.0	0.06000	0.18605
0.255	1540.0	0.07700	0.26305
0.265	1786.0	0.08930	0.35235
0.275	2015.0	0.10075	0.45310
0.285	2159.0	0.10795	0.56105
0.295	2032.0	0.10160	0.66265
0.305	1849.0	0.09240	0.75505
0.315	1488.0	0.07440	0.82945
0.325	1299.0	0.06495	0.89440
0.335	861.0	0.04305	0.93745
0.345	581.0	0.02905	0.96650
0.355	345.0	0.01725	0.98375
0.365	185.0	0.00925	0.99300
0.375	95.0	0.00475	0.99775
0.385	30.0	0.00150	0.99925
0.395	9.0	0.00045	0.99970
0.405	4.0	0.00020	0.99990
0.415	1.0	0.00005	0.99995
0.425	1.0	0.00005	1.00000

TABLE XXIV

IMPROVED WATERFLOOD LOG-INJECT-LOG ZONE 2 WORST CASE

MONTE CARLO SIMULATION
OF THE
WATERFLOOD LIL

PARAMETER	DISTRIBUTION TYPE *	RANGE OF VALUES HIGH	AVERAGE	LOW
POROSITY	0	0.345	0.325	0.305
SIGMA-BULK 1	0	17.523	16.908	16.293
SIGMA-BULK 2	0	27.356	26.639	25.922
SIGMA-WATER 1	0	32.468	31.532	30.596
SIGMA-WATER 2	0	75.559	73.387	71.215

* 0=UNIFORM, 1=TRIANGULAR

SUMMARY STATISTICS BASED ON 20000 TRIALS

NUMBER OF OBSERVATIONS	20000.0
AVERAGE SATURATION	0.2828
VARIANCE	0.0028
STANDARD DEVIATION	0.0528

SUMMARY OF OBSERVATIONS

MID-POINT	FREQUENCY	RELATIVE FREQUENCY	CUMULATIVE FREQUENCY
0.105	3.0	0.00015	0.00015
0.115	8.0	0.00040	0.00055
0.125	15.0	0.00075	0.00130
0.135	32.0	0.00160	0.00290
0.145	59.0	0.00295	0.00585
0.155	94.0	0.00470	0.01055
0.165	145.0	0.00725	0.01780
0.175	203.0	0.01015	0.02795
0.185	308.0	0.01540	0.04335
0.195	406.0	0.02030	0.06365
0.205	520.0	0.02600	0.08965
0.215	716.0	0.03580	0.12545
0.225	802.0	0.04010	0.16555
0.235	931.0	0.04655	0.21210
0.245	1116.0	0.05580	0.26790
0.255	1277.0	0.06385	0.33175
0.265	1328.0	0.06640	0.39815
0.275	1411.0	0.07055	0.46870
0.285	1509.0	0.07545	0.54415
0.295	1423.0	0.07115	0.61530
0.305	1407.0	0.07035	0.68565
0.315	1253.0	0.06265	0.74830
0.325	1164.0	0.05820	0.80650
0.335	969.0	0.04845	0.85495
0.345	855.0	0.04275	0.89770
0.355	643.0	0.03215	0.92985
0.365	508.0	0.02540	0.95525
0.375	360.0	0.01800	0.97325
0.385	237.0	0.01185	0.98510
0.395	154.0	0.00770	0.99280
0.405	88.0	0.00440	0.99720
0.415	41.0	0.00205	0.99925
0.425	9.0	0.00045	0.99970
0.435	5.0	0.00025	0.99995
0.445	1.0	0.00005	1.00000

TABLE XXV

IMPROVED WATERFLOOD LOG-INJECT-LOG ZONE 3 BEST CASE

MONTE CARLO SIMULATION
OF THE
WATERFLOOD LIL

PARAMETER	DISTRIBUTION TYPE *	RANGE OF VALUES HIGH	AVERAGE	LOW
POROSITY	1	0.345	0.325	0.305
SIGMA-BULK 1	1	17.126	16.588	16.050
SIGMA-BULK 2	1	29.405	28.580	27.755
SIGMA-WATER 1	1	32.468	31.532	30.596
SIGMA WATER 2	1	75.559	73.387	71.215

* 0=UNIFORM, 1=TRIANGULAR

SUMMARY STATISTICS BASED ON 20000 TRIALS

NUMBER OF OBSERVATIONS	20000.0
AVERAGE SATURATION	0.1172
VARIANCE	0.0018
STANDARD DEVIATION	0.0419

SUMMARY OF OBSERVATIONS

MID-POINT	FREQUENCY	RELATIVE FREQUENCY	CUMULATIVE FREQUENCY
0.0	51.0	0.00255	0.00255
0.005	66.0	0.00330	0.00585
0.015	108.0	0.00540	0.01125
0.025	188.0	0.00940	0.02065
0.035	285.0	0.01425	0.03490
0.045	470.0	0.02350	0.05840
0.055	665.0	0.03325	0.09165
0.065	882.0	0.04410	0.13575
0.075	1093.0	0.05465	0.19040
0.085	1336.0	0.06680	0.25720
0.095	1583.0	0.07915	0.33635
0.105	1754.0	0.08770	0.42405
0.115	1893.0	0.09465	0.51870
0.125	1881.0	0.09405	0.61275
0.135	1761.0	0.08805	0.70080
0.145	1523.0	0.07615	0.77695
0.155	1311.0	0.06555	0.84250
0.165	1055.0	0.05275	0.89525
0.175	799.0	0.03995	0.93520
0.185	546.0	0.02730	0.96250
0.195	358.0	0.01790	0.98040
0.205	201.0	0.01005	0.99045
0.215	114.0	0.00570	0.99615
0.225	46.0	0.00230	0.99845
0.235	19.0	0.00095	0.99940
0.245	7.0	0.00035	0.99975
0.255	4.0	0.00020	0.99995
0.275	1.0	0.00005	1.00000

TABLE XXVI

IMPROVED WATERFLOOD LOG-INJECT-LOG ZONE 3 WORST CASE

MONTE CARLO SIMULATION
OF THE
WATERFLOOD LIL

PARAMETER	DISTRIBUTION TYPE *	RANGE OF VALUES HIGH	AVERAGE	LOW
POROSITY	0	0.345	0.325	0.305
SIGMA-BULK 1	0	17.126	16.588	16.050
SIGMA-BULK 2	0	29.405	28.580	27.755
SIGMA-WATER 1	0	32.468	31.532	30.596
SIGMA-WATER 2	0	75.559	73.387	71.215

* 0=UNIFORM, 1=TRIANGULAR

SUMMARY STATISTICS BASED ON 20000 TRIALS

NUMBER OF OBSERVATIONS	20000.0
AVERAGE SATURATION	0.1168
VARIANCE	0.0034
STANDARD DEVIATION	0.0582

SUMMARY OF OBSERVATIONS

MID-POINT	FREQUENCY	RELATIVE FREQUENCY	CUMULATIVE FREQUENCY
0.0	563.0	0.02815	0.02815
0.005	232.0	0.01160	0.03975
0.015	376.0	0.01880	[illegible]
0.025	452.0	0.02260	0.08115
0.035	566.0	0.02830	0.10945
0.045	621.0	0.03105	0.14050
0.055	771.0	0.03855	0.17905
0.065	870.0	0.04350	0.22255
0.075	987.0	0.04935	0.27190
0.085	1127.0	0.05635	0.32825
0.095	1205.0	0.06025	0.38850
0.105	1227.0	0.06135	0.44985
0.115	1257.0	0.06285	0.51270
0.125	1340.0	0.06700	0.57970
0.135	1260.0	0.06300	0.64270
0.145	1193.0	0.05965	0.70235
0.155	1127.0	0.05635	0.75870
0.165	1006.0	0.05030	0.80900
0.175	855.0	0.04275	0.85175
0.185	769.0	0.03845	0.89020
0.195	631.0	0.03155	0.92175
0.205	492.0	0.02460	0.94635
0.215	387.0	0.01935	0.96570
0.225	271.0	0.01355	0.97925
0.235	174.0	0.00870	0.98795
0.245	112.0	0.00560	0.99355
0.255	83.0	0.00415	0.99770
0.265	29.0	0.00145	0.99915
0.275	10.0	0.00050	0.99965
0.285	3.0	0.00015	0.99980
0.295	3.0	0.00015	0.99995
0.305	1.0	0.00005	1.00000

TABLE XXVII

WATERFLOOD LOG-INJECT-LOG POROSITY SENSITIVITY

MONTE CARLO SIMULATION
OF THE
WATERFLOOD LIL

PARAMETER	DISTRIBUTION TYPE *	RANGE OF VALUES HIGH	AVERAGE	LOW
POROSITY	0	0.345	0.325	0.305
SIGMA-BULK 1	0	18.509	18.070	17.631
SIGMA-BULK 2	0	27.356	26.639	25.922
SIGMA-WATER 1	0	32.468	31.532	30.596
SIGMA-WATER 2	0	75.559	73.387	71.215

* 0=UNIFORM, 1=TRIANGULAR

SUMMARY STATISTICS BASED ON 20000 TRIALS

NUMBER OF OBSERVATIONS	20000.0
AVERAGE SATURATION	0.3684
VARIANCE	0.0022
STANDARD DEVIATION	0.0468

SUMMARY OF OBSERVATIONS

MID-POINT	FREQUENCY	RELATIVE FREQUENCY	CUMULATIVE FREQUENCY
0.215	5.0	0.00025	0.00025
0.225	13.0	0.00065	0.00090
0.235	25.0	0.00125	0.00215
0.245	52.0	0.00260	0.00475
0.255	118.0	0.00590	0.01065
0.265	166.0	0.00830	0.01895
0.275	265.0	0.01325	0.03220
0.285	389.0	0.01945	0.05165
0.295	534.0	0.02670	0.07835
0.305	727.0	0.03635	0.11470
0.315	882.0	0.04410	0.15880
0.325	1055.0	0.05275	0.21155
0.335	1223.0	0.06115	0.27270
0.345	1501.0	0.07505	0.34775
0.355	1494.0	0.07470	0.42245
0.365	1613.0	0.08065	0.50310
0.375	1677.0	0.08385	0.58695
0.385	1542.0	0.07710	0.66405
0.395	1492.0	0.07460	0.73865
0.405	1278.0	0.06390	0.80255
0.415	1152.0	0.05760	0.86015
0.425	888.0	0.04440	0.90455
0.435	728.0	0.03640	0.94095
0.445	476.0	0.02380	0.96475
0.455	349.0	0.01745	0.98220
0.465	187.0	0.00935	0.99155
0.475	110.0	0.00550	0.99705
0.485	47.0	0.00235	0.99940
0.495	8.0	0.00040	0.99980
0.505	3.0	0.00015	0.99995
0.515	1.0	0.00005	1.00000

TABLE XXVIII

WATERFLOOD LOG-INJECT-LOG POROSITY SENSITIVITY

MONTE CARLO SIMULATION
OF THE
WATERFLOOD LIL

PARAMETER	DISTRIBUTION TYPE *	RANGE OF VALUES HIGH	AVERAGE	LOW
POROSITY	0	0.325	0.305	0.285
SIGMA-BULK 1	0	18.509	18.070	17.631
SIGMA-BULK 2	0	27.356	26.639	25.922
SIGMA-WATER 1	0	32.468	31.532	30.596
SIGMA-WATER 2	0	75.559	73.387	71.215

* 0=UNIFORM, 1=TRIANGULAR

SUMMARY STATISTICS BASED ON 20000 TRIALS

NUMBER OF OBSERVATIONS	20000.0
AVERAGE SATURATION	0.3269
VARIANCE	0.0026
STANDARD DEVIATION	0.0506

SUMMARY OF OBSERVATIONS

MID-POINT	FREQUENCY	RELATIVE FREQUENCY	CUMULATIVE FREQUENCY
0.155	1.0	0.00005	0.00005
0.165	6.0	0.00030	0.00035
0.175	17.0	0.00085	0.00120
0.185	33.0	0.00165	0.00285
0.195	53.0	0.00265	0.00550
0.205	110.0	0.00550	0.01100
0.215	157.0	0.00785	0.01885
0.225	242.0	0.01210	0.03095
0.235	324.0	0.01620	0.04715
0.245	480.0	0.02400	0.07115
0.255	623.0	0.03115	0.10230
0.265	713.0	0.03565	0.13795
0.275	963.0	0.04815	0.18610
0.285	980.0	0.04900	0.23510
0.295	1251.0	0.06255	0.29765
0.305	1401.0	0.07005	0.36770
0.315	1381.0	0.06905	0.43675
0.325	1504.0	0.07520	0.51195
0.335	1556.0	0.07780	0.58975
0.345	1451.0	0.07255	0.66230
0.355	1360.0	0.06800	0.73030
0.365	1232.0	0.06160	0.79190
0.375	1087.0	0.05435	0.84625
0.385	893.0	0.04465	0.89090
0.395	756.0	0.03780	0.92870
0.405	534.0	0.02670	0.95540
0.415	362.0	0.01810	0.97350
0.425	259.0	0.01295	0.98645
0.435	44.0	0.00720	0.99365
0.445	87.0	0.00435	0.99800
0.455	30.0	0.00150	0.99950
0.465	6.0	0.00030	0.99980
0.475	3.0	0.00015	0.99995
0.485	1.0	0.00005	1.00000

TABLE XXIX

WATERFLOOD LOG-INJECT-LOG POROSITY SENSITIVITY

MONTE CARLO SIMULATION
OF THE
WATERFLOOD LIL

PARAMETER	DISTRIBUTION TYPE *	RANGE OF VALUES HIGH	AVERAGE	LOW
POROSITY	0	0.365	0.345	0.325
SIGMA-BULK 1	0	18.309	18.070	17.631
SIGMA-BULK 2	0	27.356	26.639	25.922
SIGMA-WATER 1	0	32.468	31.532	30.596
SIGMA-WATER 2	0	75.559	73.387	71.215

* 0=UNIFORM, 1=TRIANGULAR

SUMMARY STATISTICS BASED ON 20000 TRIALS

NUMBER OF OBSERVATIONS	20000.0
AVERAGE SATURATION	0.4051
VARIANCE	0.0019
STANDARD DEVIATION	0.0436

SUMMARY OF OBSERVATIONS

MID-POINT	FREQUENCY	RELATIVE FREQUENCY	CUMULATIVE FREQUENCY
0.265	7.0	0.00035	0.00035
0.275	18.0	0.00090	0.00125
0.285	43.0	0.00215	0.00340
0.295	84.0	0.00420	0.00760
0.305	151.0	0.00755	0.01515
0.315	239.0	0.01195	0.02710
0.325	369.0	0.01845	0.04555
0.335	554.0	0.02770	0.07325
0.345	769.0	0.03845	0.11170
0.355	940.0	0.04700	0.15870
0.365	1121.0	0.05605	0.21475
0.375	1340.0	0.06700	0.28175
0.385	1628.0	0.08140	0.36315
0.395	1623.0	0.08115	0.44430
0.405	1821.0	0.09105	0.53535
0.415	1680.0	0.08400	0.61935
0.425	1667.0	0.08335	0.70270
0.435	1471.0	0.07355	0.77625
0.445	1330.0	0.06650	0.84275
0.455	1024.0	0.05120	0.89395
0.465	822.0	0.04110	0.93505
0.475	545.0	0.02725	0.96230
0.485	384.0	0.01920	0.98150
0.495	203.0	0.01015	0.99165
0.505	118.0	0.00590	0.99755
0.515	39.0	0.00195	0.99950
0.525	6.0	0.00030	0.99980
0.535	4.0	0.00020	1.00000

APPENDIX C

NOMENCLATURE

a - cementation intercept

A - area

B_g - gas formation volume factor

B_o - oil formation volume factor

B_w - water formation volume factor

c - isothermal compressibility

C - tracer concentration

F - formation factor

h - thickness

k - permeability

k_r - relative permeability

L - neutron lifetime

m - slope of linear portion of pressure analysis plots

m - cementation factor

m - ratio of gas cap volume to oil leg volume

n - saturation exponent

N - stock tank oil initially in place

N - number of neutrons

N_p - cumulative oil production

N_r - stock tank oil remaining in place p - pressure

q - flow rate

r - well radius

R_o - resistivity of a formation at 100% water saturation

R_p - cumulative gas oil ratio

R_s - solution gas oil ratio

R_t - true formation resistivity

R_w - formation water resistivity

S - saturation

t - time

T - time

V - volume

V - velocity

W_e - cumulative water influx

W_p - cumulative water production

GREEK LETTERS

Δ - change in

μ - viscosity

Σ - capture cross section

ϕ - pore volume

SUBSCRIPTS

d - dimensionless

e - effective

f - formation

hc - hydrocarbon

i - initial

m - match

ma - matrix

o - oil

sh - shale

t - total

w - water